Georgia Institute of Technology

NASA

PHAROS

Shedding Light on the Near-Earth Asteroid Apophis

ESMD Space Grant Systems Engineering Paper Competition ▪ April 30, 2007

BLASST Space Systems

Georgia Institute of Technology

PROJECT PHAROS

Mission Overview

The *Pharos* mission to asteroid Apophis provides the first major opportunity to enhance orbital state and scientific knowledge of the most threatening Earth-crossing asteroid that has ever been tracked. *Pharos* aims to accomplish concrete and feasible orbit determination and scientific objectives while achieving balance among mission cost, risk, and schedule. Similar to its ancient Egyptian namesake, *Pharos* acts as a beacon shedding light not only on the physical characteristics of Apophis, but also on its state as it travels through the solar system.

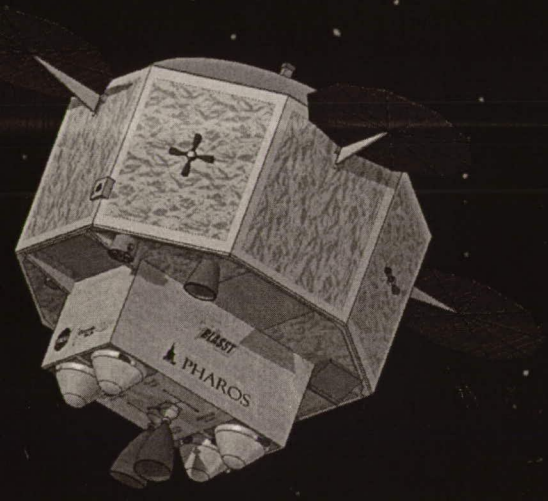

BLASST Space Systems

Launch

Delta II 7925H
C3 = 21-25 km²/s²
20-day window
in April-May 2013

Arrival

233-309 day cruise
Relative vel. <1 km/s
Hover modes at
500 m and 1000 m
distance through 2016

Science Objectives

Pharos' science objectives align with NASA Solar System Roadmap goals, including the identification of hazards to Earth and understanding the origin of the solar system's minor bodies. To meet these NASA goals, *Pharos* characterizes Apophis in each of the following areas:

1. Orbital State Vector
2. Composition
3. Mass Properties
4. Surface Mapping
5. Re-Radiation Dynamics
6. Elasticity & Coherence
7. Debris Environment
8. Energy Properties

Spacecraft Subsystems

- Dual Mode N_2O_4/N_2H_4 Bipropellant Propulsion
- Ultraflex 175 Advanced Solar Arrays
- Li-Ion Battery Storage
- State-of-the-Art AutoNav Guidance
- Fault Tolerant Propulsion, Communications, Power, and ADCS Systems

Spacecraft Mass Breakdown

Payload	62.4 kg
Spacecraft Subsystems	319.4 kg
Dry Mass	381.8 kg
Propellant	294.1 kg
Loaded Mass	675.9 kg
Adapter	45.4 kg
Boosted Mass	721.3 kg
Total Margin	198.2 kg
Launch Capability of LV	919.5 kg

Project Phase Schedule

FY07	FY08	FY09	FY10	FY11	FY12	FY13	FY14	FY15	FY16	FY17
Pre-Phase A	Phase A	Phase B	Phase C	Phase D				Phase E		

PHAROS

BLASST Space Systems

Spacecraft Bus Payloads

Instruments	Mass	Power	Function
Multi-Spectral Imager	9.6 kg	8.3 W	Determines Size/ Shape- Takes images
Near Infrared Spectrometer	15.2 kg	15.1W	Determines distribution and abundance of minerals
Near Laser Rangefinder	5 kg	16.5 W	Maps terrain- Determines rotation
Magnetometer	1.5 kg	1.5 W	Maps magnetic field

Deep Space Network (DSN) Tracking Infrastructure

An important distinction between *Pharos* and other asteroid missions is its emplacement of navigational assets at Apophis, allowing a very precise orbit determination by 2016. With the trajectory predicted to pass closer than geostationary orbit on Apophis' 2029 flyby, there is a small probability that the flyby will result in a 2036 Earth impact.

With the Deep Space Network (DSN) capable of determining range and range-rate to 1 m and 1 mm/s, weekly tracking of *Pharos* allows Apophis' state to be processed via a Kalman filter. The use of the Kalman filter reduces the error in Apophis state estimates, resulting in a best estimated trajectory which is continuously updated by the *Pharos* science team.

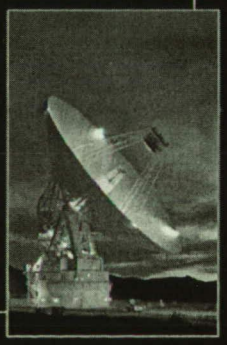

BUOI Probes

Through the Ballistic Unit and Operational Impactor (BUOI) probes, detailed orbit determination and valuable science data can be obtained. Four 7.0 kg probes will impact the surface of Apophis over a period of two weeks. Each is equipped with a set of accelerometers and temperature sensors to measure kinetic and thermal dynamic responses to an impact of up to 100 m/s.

Each probe's instrumentation set contains a highly sensitive accelerometer to measure seismic effects of successive probe impacts, allowing insight into the internal structure of Apophis. Ejecta of each impact is also monitored by *Pharos* to determine composition of the subsurface.

The probes are projected to continue to provide temperature data and act as reference beacons for over a month.

Cost Schedule

	Cost (FY07$M)
Phase A	$ 2.0
Phase B	$ 51.4
Phase C/D	$206.7
Phase E	$ 69.3
Launch	$100.1
Total	$429.5

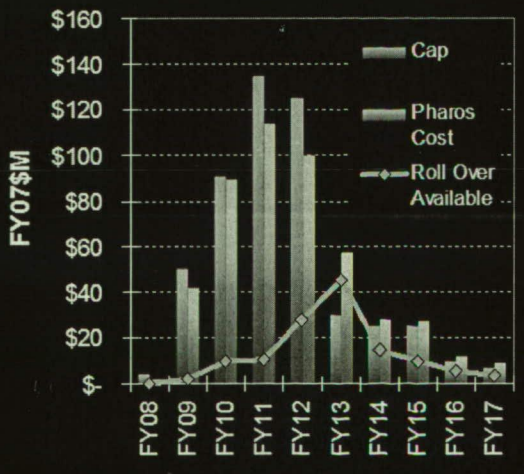

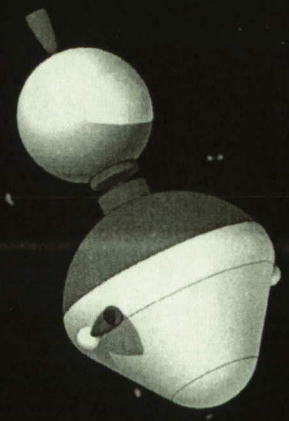

BLASST Space Systems

Jonathan Sharma, Project Manager
Jarret Lafleur, Lead Systems Engineer
Nilesh Shah, Orbit Determination Specialist
Jillian Apa, Science Payload Specialist
Jonathan Townley, Mission Systems Engineer
Kreston Barron, Spacecraft Systems Engineer

1. Executive Summary

Pharos was created by BLASST Space Systems for the second of two senior Space Systems Design courses at the Georgia Institute of Technology. Of the five teams who completed projects, BLASST was chosen to represent the class in the NASA Exploration Systems Mission Directorate (ESMD) Space Grant Systems Engineering Paper Competition. The team consists of Jonathan Sharma (Program Manager), Jarret Lafleur (Lead Systems Engineer), Kreston Barron (Spacecraft Systems Engineer), Jonathan Townley (Mission Systems Engineer), Nilesh Shah (Orbit Determination Payload Specialist), and Jillian Apa (Science Payload Specialist).

The term *Pharos* arises from the Seventh Wonder of the Ancient World, the Lighthouse at Alexandria. Just as a lighthouse sheds light on hazardous rocks at sea, *Pharos* sheds light on the looming near-Earth asteroid Apophis. The overriding goal of *Pharos* is to determine the state vector of Apophis to a degree of accuracy such that its passage relative to a critical 610 m wide keyhole at its 2029 Earth approach is known. This keyhole is outlined by Dr. Steven Chesley in his paper "Potential impact detection for Near-Earth asteroids: the case of 99942 Apophis (2004 MN4)."

In addition to orbit determination, *Pharos* incorporates key NASA Solar System Exploration Roadmap goals into its science goals. The prime spacecraft science payload includes four heritage remote sensing instruments from the 1996-2001 NEAR-Shoemaker mission and four impactor probes.

Critical to the design of the *Pharos* concept was its use of systems engineering methods and tools. Along with using tried-and-true systems engineering methods from standard space design sources, BLASST also developed its own value-based downselection process to zero in on an initial point design. Systems engineering methods were used, among other things, to determine the baseline architecture (Section 7), optimize the spacecraft subsystems (Section 8.2), and even determine the best launch dates (Section 9). In addition to systems engineering, this report includes the methods behind sizing the spacecraft (Section 8.1), determining proximity operations around Apophis (Section 9.4), and analyzing cost and risk for the project (Section 10). The Appendices include WBS and cost tables along with figures of the *Pharos* spacecraft.

2. Acknowledgements

BLASST Space Systems would like to thank the following experts in academia, government, and industry for their support and advice throughout this project:

Mr. Russell Schweickart	B612 Foundation
Dr. Steven Squyres	Cornell University
Dr. Marco Delbo	European Space Agency
Dr. George P. Burdell	Georgia Institute of Technology
Mr. Gregory Lantoine	Georgia Institute of Technology
Ms. Catherine Silvestri	Georgia Institute of Technology
Dr. Ralph Lorenz	Johns Hopkins University Applied Physics Laboratory
Dr. Richard Binzel	Massachusetts Institute of Technology
Dr. David Williams	NASA Goddard Space Flight Center
Dr. Steven Chesley	NASA Jet Propulsion Laboratory
Dr. Paul Chodas	NASA Jet Propulsion Laboratory
Mr. Ravi Prakash	NASA Jet Propulsion Laboratory
Ms. Carolyn Tewksbury	Smith College
Mr. A.C. Charania	SpaceWorks Engineering, Inc.
Dr. John Lewis	University of Arizona
Dr. James Richardson	University of Arizona
Dr. Chris Russell	University of California, Los Angeles
Dr. Daniel Scheeres	University of Michigan
Dr. David Catling	University of Washington
Dr. Juan Cruz	Georgia Institute of Technology
Dr. David Spencer	NASA Jet Propulsion Laboratory
Mr. Henry Wright	NASA Langley Research Center
Dr. John Olds	SpaceWorks Engineering, Inc.
Dr. Robert Braun	Georgia Institute of Technology
Dr. Joseph Saleh	Georgia Institute of Technology
Mr. John Christian	Georgia Institute of Technology
Mr. Kevin Flaherty	Georgia Institute of Technology

3. Table of Contents

4. Nomenclature

AR	ATLO Readiness Review
ADCS	Attitude Determination and Control System
AHP	Analytical Hierarchy Process
AI	Artificial Intelligence
AMC	Advanced Microcontroller
AO	Announcement of Opportunity
ATLO	Assembly, Test and Launch Operations
AU	Astronomical Unit
BER	Bit Error Rate
bps	bits per second
BUOI	Ballistic Unit and Operational Impactor
C	Celsius
C&DH	Command and Data Handling
CD	Compact Disc
CDR	Critical Design Review
DS2	Deep Space 2
DSN	Deep Space Network
DSS	Distributed Sensor System
E/PO	Education and Public Outreach
E_b	Energy-per-bit
EOL	End of Life
ESMD	Exploration Systems Mission Directorate
FHA	Functional Hazard Assessment
FHA	Functional Hazard Assessment
FY	Fiscal Year
GaAs	Gallium Arsenide
GDS	Ground Data System
GE	Germanium
GHz	Gigahertz
G_t	Transmit Antenna Gain
HBCU	Historically Black Colleges and Universities
HGA	High-Gain Antenna
I20	Instrument-to-Objectives
ICR	Initial Confirmation Review
InGaAs	Indium-Gallium Arsenide
I_{sp}	Specific Impulse
JPL	Jet Propulsion Laboratory
JSC	Johnson Space Center
Ka-Band	Kurtz-above band
kb	kilobits
kbps	kilobits per second
L_aL_r	Atmospheric and Rain Loss
LGA	Low-Gain Antenna
Li-$SOCl_2$	Lithium thionyl-chloride
L_l	Line Loss
L_p	Pointing Loss
L_s	Free Space Path Loss
LV	Launch Vehicle
MAG	Magnetometer
MB	Megabits
MLI	Multilayer insulation
MMRTG	Multi-Mission Radioisotope thermoelectric Generator
MOS	Margin of Safety
MRR	Mission Readiness Review
MSI	Multi-Spectral Imager
N_2H_4	Hydrazine
N_2O_4	Nitrogen Tetroxide
NASA	National Aeronautics and Space Administration
Nd-YAG	Neodymium–Yttrium–Aluminum–Garnet
NEAR	Near Earth Asteroid Rendezvous
NiCd	Nickel Cadmium
NiH_2	Nickel Hydrogen
NIS	NEAR Infrared Spectrometer
NLR	NEAR Laser Rangefinder
N_o	Noise-density
Ops	Operations
ORR	Operations Readiness Review

OSMA	Office of Safety and Mission Assurance
PDR	Product Design Review
PI	Principal Investigator
PRA	Probabilistic Risk Assessment
QFD	Quality Function Deployment
RBD	Reliability Block Diagram
RCS	Reentry Control System
RTG	Radioisotope thermoelectric Generator
S&MA	Safety and Mission Assurance
S/C	Spacecraft
SEMAA	Science, Engineering, Mathematics, and Aerospace Academy
SMAD	Space Mission Analysis and Design
SSE	Solar System Exploration
SVLCM	Spacecraft/Vehicle Level Cost Model
TCM	Trajectory Correction Maneuver
TCS	Thermal Control System
TMC	Total Mission Cost
TRK	Tracking Data Type
UHF	Ultra High Frequency
WeLCCM	Web-Based Life Cycle Cost Model

5. Introduction

The *Pharos* mission to the near-Earth asteroid Apophis provides humankind with its first major opportunity to enhance the orbital state and scientific knowledge of the most threatening Earth-crossing asteroid that has ever been tracked. Following the goals of the NASA Solar System Roadmap, *Pharos* will advance the current state of knowledge of near-Earth Asteroids while helping to lead the way towards future manned missions.

This proposal presents BLASST Space Systems' plan to implement *Pharos*, which aims to accomplish concrete and feasible orbit determination and scientific objectives while achieving balance among mission cost, risk, and schedule. Named for the ancient lighthouse at Alexandria, *Pharos* acts as a beacon shedding light not only on physical aspects of Apophis, but also on its orbital state as it travels through the solar system.

The asteroid Apophis was discovered in June 2004 and observed again in December of that year. Within a week the asteroid's impact risk reached an unprecedented level of 4 on the Torino Scale for an impact on April 13, 2029. Since 2004, observations and analysis have eliminated the possibility of a 2029 impact, but the small probability (2.2×10^{-5}) of a 2036 impact still exists. Consequences of an impact would be regional-scale destruction. An impact in the Gulf of Mexico, for example, could produce tsunami peak run-ups of over 30 meters (98 feet). Infrastructure losses alone have been estimated at over $400 billion.

Table 5.1. The prime impetus behind *Pharos* is the effect that current uncertainty in Apophis' physical and orbital characteristics have on 2036 Earth impact predictions.

Parameter	Value	Unit	Comment
Physical Characteristics			
Asteroid Type	Q		Uncommon
Abs. Magnitude	19.7		±0.2
Rotation Period	30.40	hr	+0.01 / -14.1 hr
Albedo	0.33		±0.04
Length	270	m	+20 / -30 m
Width	190	m	+10 / -20 m
Height	160	m	+10 / -20 m
Mass	21	Tg	+42 / -14 Tg
Orbital Characteristics *(Epoch at 2007-04-10.0)*			
Semimajor Axis	0.922	AU	$\pm 2.4\times10^{-8}$ AU
Eccentricity	0.191		$\pm 7.6\times10^{-8}$
Inclination	3.33	deg	$\pm 2.0\times10^{-6}$ deg
Asc. Node	204.5	deg	$\pm 1.1\times10^{-4}$ deg
Arg. Perih.	126.4	deg	$\pm 1.1\times10^{-4}$ deg
Mean Anomaly	307.4	deg	$\pm 3.2\times10^{-5}$ deg

Since 2004, Apophis and similar Earth-crossing asteroids have continued to generate interest in NASA, the UN, and advocacy groups. Most recently in 2007, headlines were made when former astronaut Rusty Schweickart updated the UN on plans for a blueprint for asteroid threat global response. In November of 2006, NASA announced its intention to use the new Constellation Program to send manned missions to explore near-Earth Objects (NEO) such as asteroids. With

this goal in mind, it is essential to obtain concrete information about possible destinations before humans are to safely explore these frontiers. Missions such as *Pharos* will be needed in the upcoming years to pave the way for future manned missions.

Current work on Apophis focuses on accurate orbit determination, which is also the overriding goal of *Pharos*. Table 5.1 shows the large uncertainties that exist in the physical and orbital characteristics of Apophis. While accurate knowledge of orbital characteristics is clearly the most critical in prediction of the asteroid's 2036 Earth pass, physical characteristics are also important due small body energy radiation effects (e.g., the Yarkovsky Effect).

In the context of NASA's Solar System Exploration (SSE) Roadmap, the *Pharos* mission objectives in Table 5.2 fall under three broad questions ranked by importance:

SSE Roadmap Question 5: What are the hazards and resources in the Solar System environment that will affect the extension of human presence in space?

Pharos' primary mission is the improvement of knowledge of Apophis' orbital and physical characteristics, both of which are critical to orbit determination and prediction of the 2036 Earth pass. As an Earth-crossing asteroid, Apophis is a hazard to human presence in space and on Earth. Additionally, *Pharos* identifies mineral or organic resources of interest to human and robotic missions to asteroids in the future. Of the eight objectives listed in Table 5.2, seven are tied to this SSE Roadmap question.

SSE Roadmap Question 1: How did the Sun's family of planets and minor bodies originate?

Studying the composition, mass properties, coherence, and other geophysical properties of Apophis lends scientific insight into the origin of this asteroid and others like it. Apophis is of particular interest because of its classification as a Q-type asteroid, a type speculated to be abundant in the solar system, but of which few examples have been discovered. Six of the eight objectives in Table 5.2 are tied to this question.

SSE Roadmap Question 3: What are the characteristics of the Solar System that led to the origin of life?

Part of *Pharos*' payload is a spectrometer which allows for the analysis of the surface composition of Apophis for the presence of organic materials. Furthermore, impactor probes allow *Pharos* to analyze subsurface composition. Six of the eight objectives in Table 5.2 are tied to this question.

As described later in this proposal, the objectives presented here are chosen based on a rigorous downselection process which couples mission objective selection with architecture selection to ensure a high scientific return for a minimum cost.

Table 5.2. *Pharos*' goals emphasize measurements which contribute to NASA SSE Roadmap objectives and enhance knowledge of parameters key to future predictions of Apophis' orbit.

Priority	Objective		Description	Instruments	NASA Obj.
1	**State Vector**	Position Velocity Acceleration	Determine state to accuracy of 1 m and 1 mm/s, via telecom	BUOI, NLR, Comm	5
2	**Composition**	Mineralogy	Map abundance of minerals within 2 m	BUOI, NIS	1,3
		Organics	Assess the presence of water	BUOI, NIS	
3	**Mass Properties**	Mass	Mass of asteroid determined to within 1% accuracy	S/C	1,5
		Size	Determine size to within 10 m	MSI	
		Shape	Determine shape to an accuracy of 1%	MSI, NLR	
		Gravity Concentrations	Gravity of asteroid determined to 1% accuracy	S/C	
4	**Mapping**	Mineral Distribution	Map mineral distribution to within 2 m	MSI, NIS	1,5
		Surface Features	Map surface features to within 0.1 m from a 1 km orbit	MSI, NIS, NLR	
5	**Re-Radiation Dynamics**	Rotation Rate	Rotation rate within .002 deg/day	BUOI, NLR	5
		Reflectivity	Measure 63 spectra to determine reflectivity	MSI, NIS	
6	**Elasticity & Coherence**	Surface Porosity	Determine extent of surface solidity	BUOI, NIS	1,5
		Internal Structure	Density to within 10%	BUOI, NIS	
7	**Debris Environment**	Ejecta Properties	Determine internal structure and near-surface composition	BUOI, MSI, NIS	1,5
		Latent Debris Field	Monitor debris field to identify hazardous probe landings	MSI	
8	**Energy Properties**	Magnetic Fields	Record magnetic fields around asteroid to a 0.1 nT range	MAG	1,5
		Temperatures	Record surface asteroid temperature to within 0.3°C	BUOI	

6. Project Requirement

The Announcement of Opportunity (AO) sets certain program and mission level requirements that must be fulfilled. The program level requirements generally involve cost and schedule. The mission has a cost cap of $500 million ($FY07) with Phase A's cost set at $2 million. The cost schedule is also set for each real year with rollover allowed. The schedule of the mission is also defined with all data returned and analyzed by December 31st, 2016. There is also a restriction of a 12-month Phase A and a 52-month Phase C/D. Education and public outreach must also be accomplished.

There are also several mission level requirements specified in the AO. Information about Apophis' orbit must be defined to a 10% confidence to justify a deflection mission decision by 2017. The mission must also provide scientific findings that support NASA's Solar System Exploration Roadmap with all information transferred to the Planetary Data System by the end of 2016. Critical events are required to be continuously monitored in order to enable reconstruction of data. Planetary protection requirements are also considered.

7. Downselection Methodology

7.1. Methodology Motivation

One of the most critical tasks in the design of complex engineering systems is the initial conversion of mission or program objectives into a integrated system to fulfill them. Moreover, a challenge exists to comprehensively explore the global design space while still leaving enough time and resources to decide upon the fine details of the selected point design. At one extreme, a comprehensive exploration of the global design space could theoretically be achieved with a monolithic vehicle or architecture model but could easily involve the complexity and unmanageability of hundreds of design variables and dozens of objectives. At the other extreme, a quick downselection based on engineering judgment is prone to reliance on historical experience and could easily produce suboptimal solutions for the problem at hand. The BLASST Space Systems downselection methodology for its *Pharos* design is believed to be a superior compromise between these two extremes which is aimed at the maximization of mission benefit-to-cost ratio. As will be seen, metrics other than mission benefit and mission cost are considered, but these two metrics are believed to be most critical to limited-budget planetary missions in general and are also the most easily estimatable variables early in design.

7.2. Methodology Summary

The full BLASST downselection method is summarized in Figure 7-1. The process begins with the definition of objectives and ends at the initiation of detailed design and subsystem trades. Thus, the process starts with a global picture of the concept design space and intelligently narrows possibilities to the space surrounding a single point design. Key aspects are summarized below, and a more detailed summary is contained in the sections that follow.

Prioritization Matrices. Objective prioritization is divided into program and mission levels. The program level contains overriding programmatic objectives such as cost, risk, and schedule, while the mission level contains mission-specific objectives (e.g., science). An Analytical Hierarchy Process (AHP) is used for prioritization.

I2O Maps. Next, candidate architectures are defined. For each candidate architecture, a Payload Instrument-to-Objectives (I2O) map is created. The I2O map is modeled in the form of a Quality Function Deployment (QFD), but differs in that it maps mission-level objectives to the ability of candidate payloads to fulfill each objective. The bottom row of the I2O map indicates how important a given payload is to the defined mission.

Cost and Importance Estimation. Potential payloads from the I2O matrices are next assorted into thousands of cases for each of the candidate architectures (10,000 cases per candidate architecture are used for the *Pharos* evaluation). For each individual case, which has a unique

payload combination, mission importance is estimated as the sum of individual payloads' importances. Cost is estimated using a variety of first-order estimation tools, including a historical mass model, ΔV estimates, launch vehicle database, and cost estimation models.

Pareto Plot and Final Downselection. After cost and importance estimates are complete, results are plotted in the importance vs. cost objective space to observe the trade via a Pareto front. Several points are chosen along the front for further evaluation in the original program-level prioritization matrix and AHP. The results of this final AHP determine the final concept.

A distinguishing feature of this overall process is its inclusion of an automated evaluation of the cost and mission importance of thousands of possible payload choices. The Pareto front shows that the final design is on the frontier of achievable mission importance-to-cost ratios. A program-level AHP prioritization matrix evaluation follows selection to ensure consideration of non-cost and non-science factors. The original cost and mass estimates from the process are quite accurate. Initial *Pharos* estimates yield a vehicle loaded mass of 706 kg and program cost of $410 million (FY07 dollars).

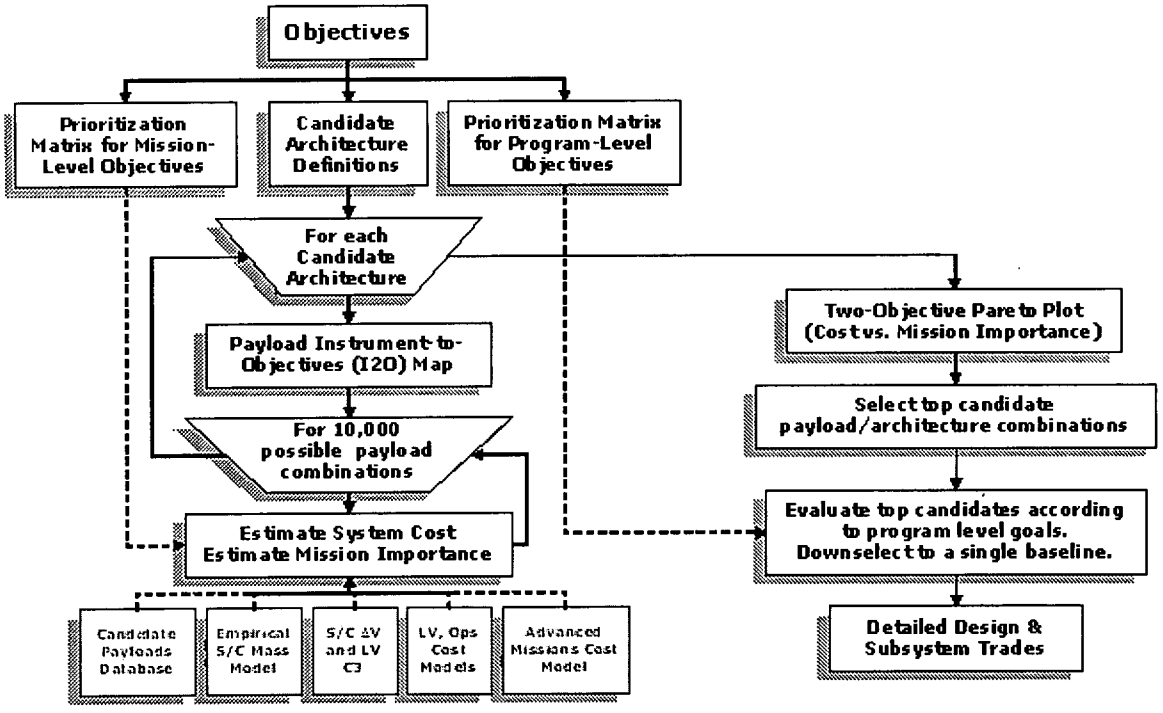

Figure 7-1. BLASST's downselection method allowed a comprehensive first-order evaluation of the *Pharos* trade space for simultaneous selection of specific objectives and architecture.

7.2.a. Objectives

The beginning of the design process is marked by recognition and documentation of formal requirements from the simulated NASA Announcement of Opportunity (AO). These requirements, discussed earlier, are summarized in Figure 7-2 below. Note that BLASST divides the requirements into both the program and mission levels, where the program level consists of aspects such as cost and schedule and the mission level consists of specific technical mission requirements.

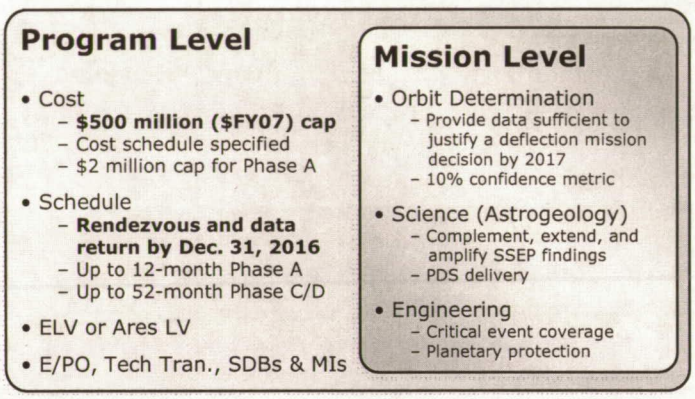

Figure 7-2. The *Pharos* design is driven at the highest level by NASA AO requirements.

7.2.b. AHP Prioritization Matrices

The program and mission level requirements given by the AO are next translated into a number of objectives for the *Pharos* mission which are prioritized in two AHP prioritization matrices. As shown in Figure 7-3, program-level objectives include aspects of cost, risk, schedule, and public demonstration of action regarding deep space technologies and near-Earth objects in general. Mission-level objectives are a subset of the program-level objectives and include specific orbit determination, science, and engineering objectives of interest.

The full prioritization matrices are shown in Figure 7-4. Mission-level priorities regarding science and orbit determination are given previously in Table 5.2. In the rightmost column of Table 5.2 are the NASA Solar System Exploration Roadmap objectives (noted earlier in this report) which each objective effectively falls under. Given the focus of the AO, it is not surprising that highest priority is placed on the precise determination of Apophis' state vector. The second priority of the mission is determination of the composition of Apophis in terms of mineralogy and any potential presence of organic materials.

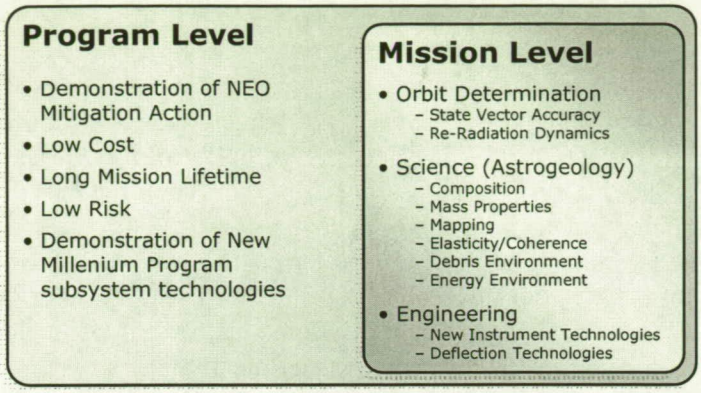

Figure 7-3. BLASST characterizes *Pharos* program and mission goals as above to allow prioritization.

Program-Level Prioritization Matrix

	Low Cost	Low Risk	Long Lifetime	Public Appeal	Orbit Determination & Science	Deflection Tech. Demo	Instrument Tech. Demo	Subsystem Tech. Demo	Priority Vector
Low Cost	1	4	7	1/4	1/6	1/2	1/3	2	0.091
Low Risk	1/4	1	1/3	1/3	1/5	1/2	1/3	2	0.042
Long Lifetime	1/7	3	1	1/6	1/7	1/2	1/3	1	0.048
Public Appeal	4	3	6	1	1/3	1	1/2	5	0.144
Orbit Determination & Science	6	5	7	3	1	5	3	7	0.368
Deflection Tech. Demo	2	2	2	1	1/5	1	1/2	4	0.099
Instrument Tech. Demo	3	3	3	2	1/3	2	1	4	0.176
Subsystem Tech. Demo	1/2	1/2	1	1/5	1/7	1/4	1/4	1	0.032

Mission-Level Prioritization Matrix

	Position/Velocity/Acceleration	Rotation & Reflectivity	Mass Properties & Distribution	Composition	Elasticity & Coherence	Radiation, Magnetism, and Temp.	Debris & Plumes	Mapping	Priority Vector
Position/Velocity/Acceleration	1	3	3	2	4	4	3	2	0.255
Rotation & Reflectivity	1/3	1	1/2	1/2	3	4	2	1	0.107
Mass Properties & Distribution	1/3	2	1	1/3	3	5	4	2	0.151
Composition	1/2	2	3	1	4	5	5	2	0.215
Elasticity & Coherence	1/4	1/3	1/3	1/4	1	3	3	1/3	0.065
Radiation, Magnetism, and Temp.	1/4	1/4	1/5	1/5	1/3	1	1/2	1/4	0.033
Debris & Plumes	1/3	1/2	1/4	1/5	1/3	2	1	1/5	0.046
Mapping	1/2	1	1/2	1/2	3	4	5	1	0.129

Figure 7-4. *Pharos* objectives are divided into program and mission level prioritization matrices as above.

7.2.c. Candidate Architecture Definitions

The next step in the BLASST downselection process is the definition of candidate mission architectures. Four core architectures are chosen for evaluation, although two additional architectural options (a sample return system and distributed sensor system) are also considered and modeled as payloads. The first candidate architecture is dubbed a two-phase orbiter/lander in which an orbiter operates in proximity to Apophis and has the capability to land and return data at end of life. The second option is a lander only for which all instrumentation is geared toward surface activity, and the third option is an orbiter only for which all instrumentation is geared toward remote sensing. The fourth candidate architecture is a separate orbiter and lander in which an orbiting mother ship launches a lander to conduct surface operations. Three additional candidate architectures are defined which are identical to the first three but which consist of twin vehicles instead of a single one.

7.2.d. Instrument-to-Objective (I2O) Maps

The final step required to enable the automated analysis of thousands of potential vehicle designs is the definition of an instrument-to-objective (I2O) map for each candidate architecture. A sample I2O map is shown in Figure 7-5. Modeled in the form of a QFD, the left two columns contain mission-level priorities from the associated prioritization matrix. The top two rows contain all payloads under consideration plus their masses. In the remaining rows and columns, each potential payload is ranked as a 1, 3, or 9 in terms of how well it fulfills the corresponding objective. The bottom row indicates each instrument's overall importance score, which is calculated from Equation 1. In Equation 1, qi is a given instrument's correlation ranking (1, 3, or 9) for a given objective i, and pi is the priority of that objective.

$$I_{instr} = \sum_i q_i p_i \tag{1}$$

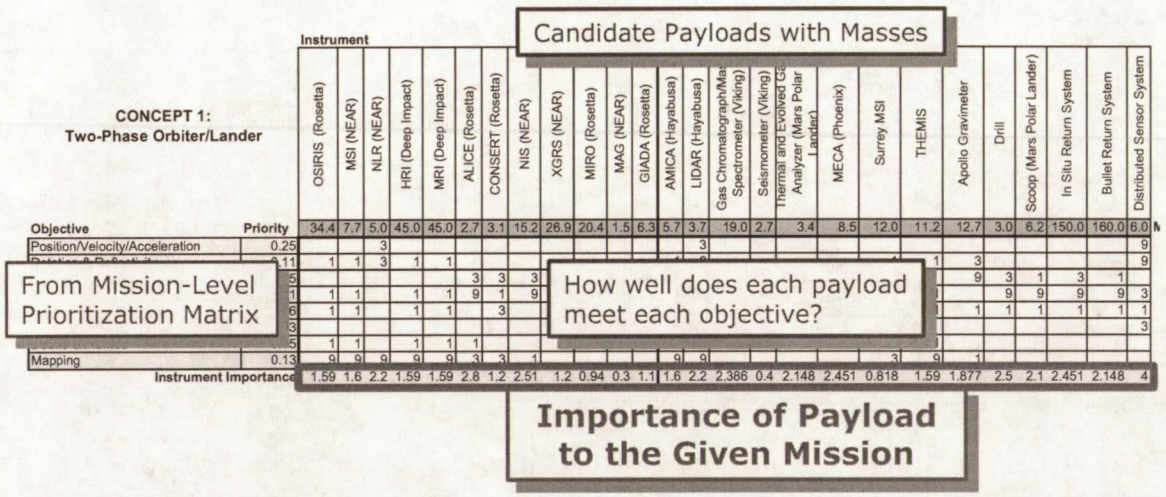

Figure 7-5. A sample Instrument-to-Objective (I2O) Map determines relative importances of all potential payloads to each *Pharos* mission candidate architecture.

7.2.e. Automated Cost and Importance Estimation

Automated cost and importance estimation is performed using a 240-line MATLAB code which takes the I2O Map payload masses and importances, generates a series of potential payload combinations (in this case, 10,000 combinations were chosen per candidate architecture), and evaluates each payload combination to determine mission cost and mass. For a given payload combination, the evaluation takes several steps:

1. ***Mission ΔV and C3 Definition.*** Outputs from a cost-based mission design process described later in this report produce approximate launch vehicle C3 and arrival ΔV values. Maintenance ΔV requirements are also estimated.

2. ***Spacecraft Dry Mass Estimation.*** Spacecraft dry mass is estimated via a historical curve fit from the total payload mass based on seven similar past missions. This is effectively a rough sizing of all spacecraft subsystems and support hardware.

3. ***Spacecraft Gross Mass Estimation.*** Spacecraft gross mass is estimated via application of the rocket equation using the estimated dry mass and the arrival and maintenance ΔV numbers from previous steps. A hypergolic engine specific impulse of 300 s is assumed.

4. ***Launch Vehicle Selection.*** With spacecraft gross (launch) mass known, a launch vehicle is selected from an in-house Georgia Tech Space Systems Design Laboratory (SSDL) launch vehicle database. The lowest-cost American launch vehicle which can lift the spacecraft to the specified C3 is automatically selected.

5. ***DDT&E Cost Estimation.*** Design, Development, Test, and Evaluation (DDT&E) cost is estimated using an Advanced Missions Cost Model scaled to produce correct DDT&E costs for the NEAR-Shoemaker mission to the asteroid Eros.

6. ***Ancillary Cost Estimation.*** Integration, Assembly, and Test (IA&T), program management, ground equipment, operations, and software costs are estimated using methods from *Space Mission Analysis and Design III* by Larson and Wertz.

From the information generated by these six steps, the total cost estimate is known, and the total mission importance is taken as the sum of the individual instrument importances.

7.2.f. Pareto Plot

From the 70,000 approximate point designs generated by the automated cost and importance evaluation, a plot can be made representing the inherent trade between cost and attainable mission importance. This plot is shown in Figure 7-6. Some important characteristics to note are the large vertical white spaces near \$350M and \$425M, discontinuities which are the result of jumps in launch vehicle. It can also be seen that all "A" concepts, or two-vehicle variants of the four core concepts, lie away from the well-populated Pareto front which forms the border between the white and populated space on the graph. This Pareto front represents the set of non-dominated solutions, or the set of solutions for which no same-cost mission has higher importance or for which no same-importance mission has lower cost. Ideally, the chosen design (at least from a cost and mission importance standpoint) will lie on the Pareto front.

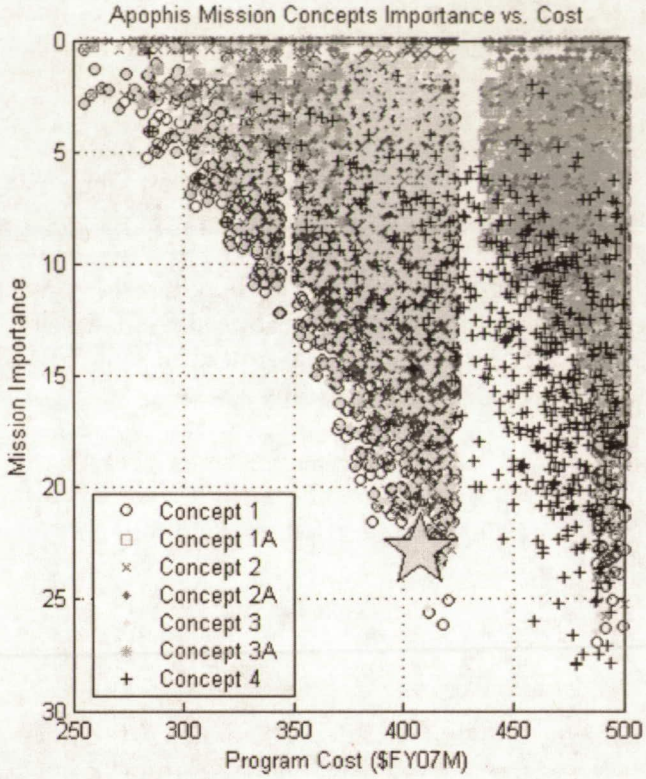

Figure 7-6. This plot showing the resulting costs and importances of thousands of potential missions to Apophis justifies the final concept and payload selection of *Pharos*, which lies at the yellow star on the Pareto front.

7.2.g. Final Candidate Architecture and Payload Selections

To continue to the final downselection of a point design, several points are selected for detailed examination from the Pareto front identified in the previous step. By examining each of these points, the BLASST team is able to learn common characteristics of the most efficient designs. One of the lowest-cost solutions on the Pareto front, for example, used only a spectrometer from the European Rosetta mission at a cost of just $250 million. Higher-cost solutions utilized multiple distributed sensors (modeled after the 1999 Mars Microprobes) plus a suite of instruments, which allowed the team to realize that the advantage of designing for a larger payload not only allowed more scientific return but also more scientific return per dollar (i.e. importance per dollar as quantified in Figure 7-6 above). Furthermore, the team noticed that most mid- and high-range Pareto-optimal solutions utilized one or more distributed sensors.

With this insight in mind, the team chose four designs to evaluate in the final program-level prioritization matrix. The first was a two-phase orbiter/lander concept with an imager, laser rangefinder, magnetometer, mass spectrometer, and four probes. The second was a variant of this concept which utilized two orbiters, each carrying half the instruments listed above. While this second option was not on the original Pareto front, it was decided to examine it since it may

have benefits in terms of lower operational risk, a characteristic not captured on the importance-cost Pareto plot. The third candidate was similar to the $250 million concept mentioned earlier, an orbiter with only a single instrument. The fourth was a large lander like one of those seen in Figure 7-6 as the black crosses in the $450M - $500M range with high (25-30) importances.

7.2.h. Final Downselection

As indicated by Figure 7-1, final downselection is conducted by evaluating the four final candidate designs via an AHP based on the program-level prioritization matrix. The results of this evaluation are shown in Table 7.1. Note that compared to the baseline Pareto-optimal two-phase orbiter/lander design mentioned above, the two-vehicle solution scored higher but was in the end not selected because of concerns that the budget would not allow (the baseline concept was already at $410 million). The minimal-instrumentation orbiter scored the lowest of all because of the heavy weighting that orbit determination and science had in the program-level priorities. The Pareto-optimal lander scored close to the baseline design, but it was also discarded due to cost concerns since it lay so close to the cost cap.

Table 7.1. Final scores of candidate designs justify the choice for the baseline Pareto-optimal two-phase orbiter/lander. Note that while the twin vehicle concept scored slightly higher, cost considerations kept it from further consideration.

Candidate Design	Final Score
Baseline Pareto-Optimal Two-Phase Orbiter/Lander	0.290
Twin Two-Phase Orbiter/Landers	0.317
Minimal-Instrumentation Pareto-Optimal Orbiter	0.114
Pareto-Optimal Lander	0.279

Thus, the final selection was the baseline two-phase orbiter/lander described above. Note that due to the payload choices for the vehicle, this is very close to an orbiter solution since end-of-life landing on an asteroid can be done with little or no dedicated landing gear, as demonstrated by the NEAR mission. Perhaps the most powerful aspect of this analysis method is that it can show that this final design lies squarely on the Pareto front of the mission importance vs. cost objective space as shown by the yellow star in Figure 7-6. This plot showing the resulting costs and importances of thousands of potential missions to Apophis justifies the final concept and payload selection of *Pharos*, which lies at the yellow star on the Pareto front.. The initial mass and cost estimate is 706 kg and $410 million (FY07 dollars), respectively. Furthermore, when to compared to the final mass and cost estimates which are the result of very detailed sizing and costing analysis (721 kg and $430 million), this initial estimate is found to be 2-5% accurate.

The resulting mission architecture which was to a large extent dictated by this final selection is shown in Figure 7-7 below. Launch and transplanetary injection takes place on a Delta II 7925H expendable launch vehicle in a launch window spanning April to May of 2013. After a cruise period, arrival occurs in late 2013 or early 2014. Proximity operations begin shortly thereafter, and the launch of the four Ballistic Unit and Operational Impactor (BUOI) probes occurs about 3 months after arrival. After 2.5 years of tracking and science operations, the *Pharos* spacecraft conducts a disposal operation whereby it sets itself on the surface of Apophis to gather images and data during descent and any brief period of surface operation.

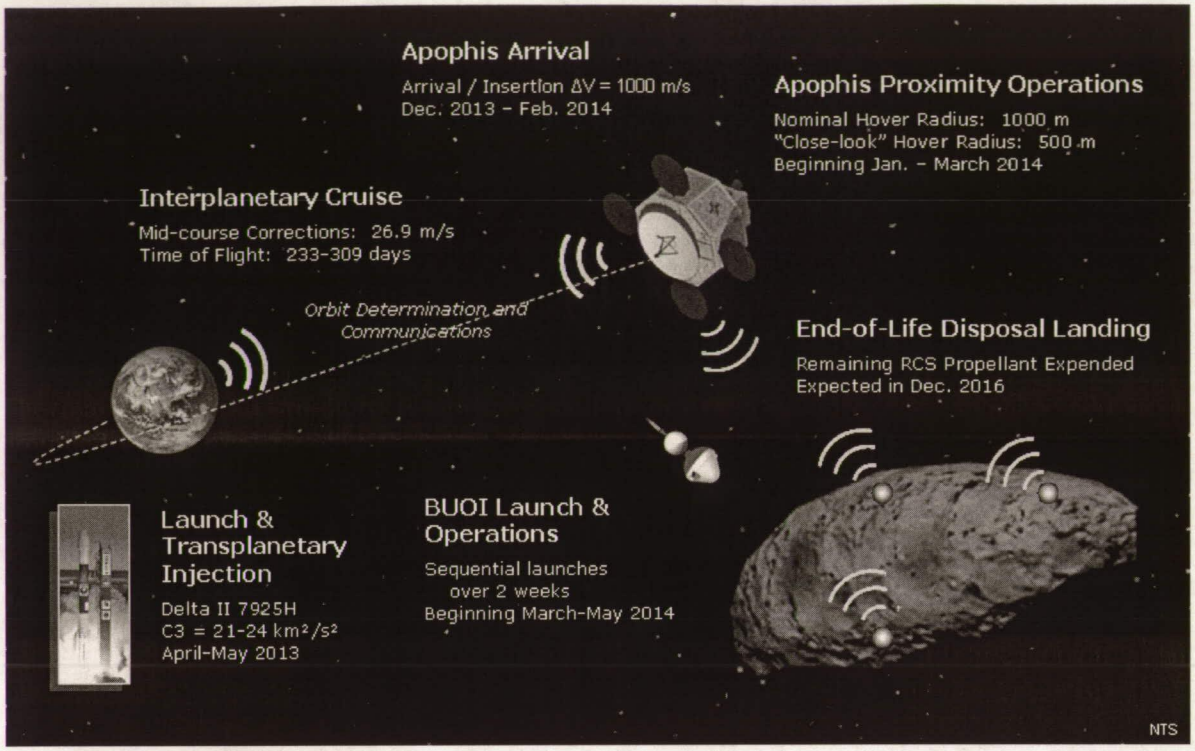

Figure 7-7. The *Pharos* mission encompasses six major operational phases to accomplish its science and orbit determination goals before the end of 2016.

8. Spacecraft Sizing and Optimization

8.1. Subsystem Sizing

8.1.a. Main Craft

The main spacecraft structure for this mission is designed as an octagonal shape. Power is provided by four solar arrays that deploy in a circular form. These multi-function solar arrays provide 696 W beginning of life (BOL) power. Secondary 435 W-hr Lithium Ion batteries are used to store excess power. The craft utilizes a high gain Ka-band parabolic antenna for communications and the instrument panels are located on the overhang of the spacecraft. The propulsion system consists of 2 main engines using nitrogen tetroxide/hydrazine (N2O4/N2H4) bipropellant, and monopropellant hydrazine (N2H4) for the 12 RCS thrusters. Spacecraft guidance is achieved through use of AutoNAV. Figure 8-1 shows a full breakdown of all subsystems.

Payload

The spacecraft's payload is comprised of four science instruments and four deployable probes. The fixed onboard science instruments consist of an Multi-Spectral Imager (MSI), a Laser Rangefinder (NLR), a Magnetometer (MAG), and a Infrared Spectrometer (NIS).

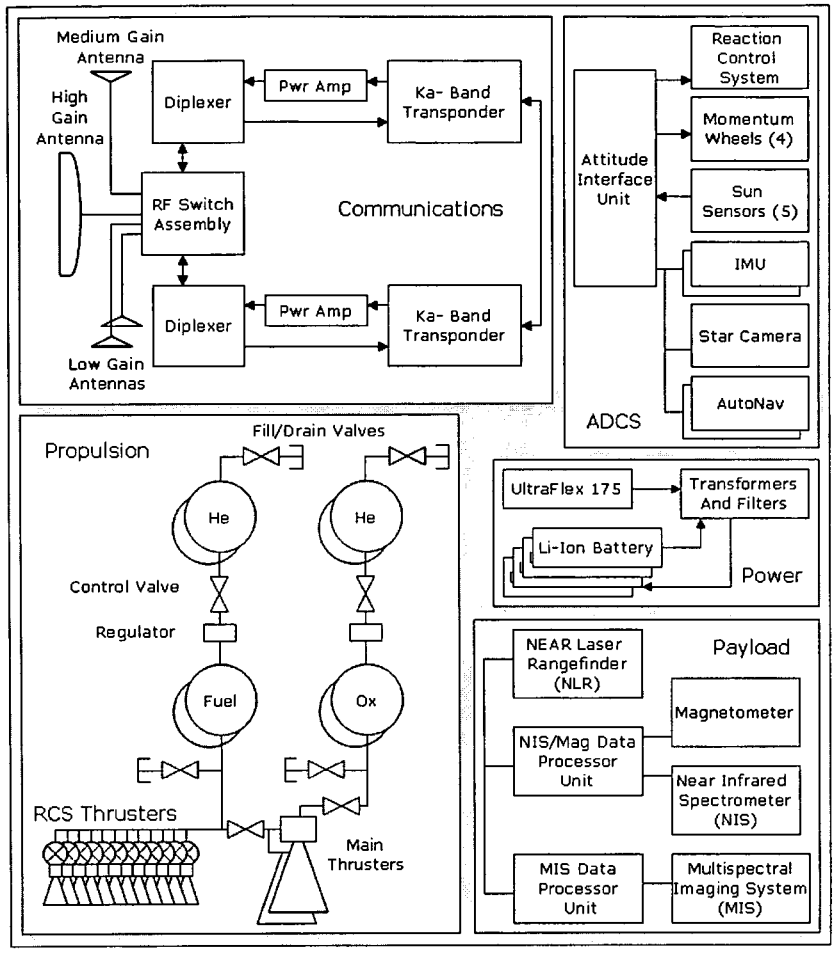

Figure 8-1. Block diagrams key components of *Pharos*' system architecture.

Propulsion

The spacecraft utilizes a dual mode nitrogen tetroxide/hydrazine (N2O4/N2H4) bipropellant for the two main engines, and monopropellant hydrazine (N2H4) for the 12 RCS thrusters. This allows for a lower mass and less complex system when compared to alternative systems. Both main engine and RCS thrusters use the same N2H4 propellant and pressurant tanks. Xenon ion engines were considered, but use of this system increases the power consumption from propulsion from 5 W to 600 W and the loaded mass by 15%. The basis for calculating the performances of the propulsion system are based off the ADLAE engine designed by TRW Inc.

Twelve RCS thrusters are used on the craft for attitude adjustments and station-keeping. The performance characteristics this RCS are based upon RCSs developed by TRW Inc. The fuel mass required for the main engine and RCS thrusters is 75.3 kg and 94.8 kg respectively, yielding a total mass in the fuel tanks of 170.1 kg.

The maintenance acceleration budget is calculated considering worst-case solar perturbations and the hover mode acceleration needed to withstand Apophis gravity. The maintenance acceleration budget is then used to calculate maintenance fuel mass and its associated ΔV. Table 8.1 shows the complete maintenance budget.

Table 8.1. Small acceleration perturbations are responsible for low ADCS mass and slewing rates.

Maintenance Acceleration Budget	(m/s^2)
Solar Perturbations	4.23E-08
Hover mode	5.00E-06
Other	0
Subtotal	5.04E-06
Margin (15%)	7.56E-07
TOTAL	5.79E-06
Total Impulse (kN-s)	217.69

Communication

The communication network for this spacecraft relies on NASA's 32 GHz Ka-band Deep Space Network (DSN). The DSN antenna arrays consist of 70 m and 34 m diameter antennas with antenna efficiencies of 60%. To communication, the spacecraft makes use of a pre-deployed parabolic main antenna with a feed array. The mass of the main antenna is calculated using a parametric sizing tool which minimizes vehicle boosted mass by trading between antenna diameter (i.e. added mass) and power system mass incurred from extra communications system power requirements. The final antenna has a diameter of 1.5 m, a transmitter efficiency of 60%, and a Gt of 133,000.

The backup antenna is a medium-gain, fanbeam antenna with a mass of 0.7 kg and an antenna efficiency of 60%. The Gt of the backup antenna is 115. The spacecraft is also outfitted with 2 hemispherical antennas located on the fore and aft ends of the spacecraft, for UHF communication with the BUOIs.

ADCS

The spacecraft attitude is controlled through 3-axis stabilization. Navigation is achieved by using a star sensor and a sun sensor and an extra four sun sensors for redundancy.

The ADCS is also comprised of a state-of-the-art real-time, space-borne navigation system known as AutoNav. Use of this system eliminates the need for post-processing and ground intervention. The AutoNav system makes use not only of the star and sun sensors, but the synchronization of optical cameras and RCS thrusters to steer. The AutoNav system constantly monitors the trajectory of the spacecraft and performs on-orbit calibrations accordingly.

To help stabilize the system, *Pharos* makes use of three momentum wheels with one extra for redundancy. The worst case disturbance torque calculated at Apophis is 5.17×10-6 N-m. Therefore the angular momentum storage for the momentum wheels in a non-orbit, hover mode

at Apophis is 3.13 N-m-s. At Apophis arrival, *Pharos* initiates a hover mode with a hover requirement of 865 m from the surface. At this height, the spacecraft rotates so the main antenna is pointing toward earth and the solar arrays are pointed toward the sun. At this point, bias and drift from plumes, debris, or deployment of the BUOIs is automatically corrected by the AutoNav system, in conjunction with the RCS thrusters and momentum wheels.

The solar array is stowed in a closed-design panel configuration before deployment. During motor-driven deployment, the lanyard is attached to the pivot panel & reeled onto motor pulley. The deployment process continues as the lanyard is further reeled onto motor pulley, unfurling the solar array in a sweeping motion. The operation continues until the pivot panel has rotated 360°. The solar array is preloaded and latched when it is fully deployed at 360°.

The only articulated devices onboard the craft are the solar arrays and the high gain antenna. The main antenna is gimbaled mechanically for earth pointing. The solar arrays can articulate about the axis perpendicular to the side they are mounted on.

C&DH

The data requirement from the payload instruments total to 13.5Mb of data demanded at 10.2kbps. Onboard are two recorders with 1 Gb of storage, with one of them serving as a backup in the event of ground test failure. The C&DH system incorporates the spacecraft subsystems with a centralized computing architecture.

Power

Power is supplied to the spacecraft using an innovative deployable solar array system, known as UltraFlex 175, capable of producing large amounts of power while also keeping a low overall spacecraft mass. UltraFlex 175 makes use of a 140-micron-thick, Triple-Junction (TJ) GaInP2/GaAs/Ge solar array. It has a specific performance of 155 W/kg, specific performance packaging efficiency of 35000 W/m3, and a power per solar array area of 310 W/m2. Because of the performance factors of the UltraFlex 175, the total power available to the spacecraft is 696 W BOL. The UltraFlex 175's light weight design yields a total mass of 4.5 kg, giving a 10% reduction in loaded spacecraft mass with respect to other solar array options. This includes a 50% redundancy in the UltraFlex 175 arrays. Using four UltraFlex 175 arrays, the total solar array area is reduced by 32% compared to using traditional GaAs solar arrays.

The spacecraft makes use of two primary and two secondary Lithium Ion batteries. Using Lithium Ion batteries reduces the spacecraft's loaded mass by 9% with respect to NiCad batteries and a 2% mass reduction compared to NiH2 batteries. The Lithium Ion batteries have a battery capacity of 435 W-hr and a battery charge power of 9.8 W. During trade studies, RTG-based power systems were considered yet added about 200 kg to the loaded mass of the spacecraft. For this particular inner solar system mission, RTG's are not necessary. In addition, these RTG's are costly to implement due to their use of nuclear reactions.

Power is controlled and regulated through the use of a Direct-Energy-Transfer (DET) system to easily dissipate power not used by the loads, making this an efficient method for power control in comparison to Peak-Power-Tracking (PPT).

Thermal and Structures

The dual active and passive thermal system for the spacecraft will utilize a combination of Multilayer insulation (MLI) blankets, heat pipes, heaters, and electronics to control the active systems. The low-emittance films and low-conductivity layers are suitable to protect the propellant lines and other sensitive equipment while the heaters protect the two propellant tanks.

The octagonal frame of the spacecraft houses all instruments and all eight onboard tanks in a simplified, integrated design. The tanks are placed in the wide base of the frame, with all electronics and instruments placed above the tanks. The mass of the structure is 23.1% of the dry mass, a value derived from empirical data.

Adapter

The adapter for this spacecraft is configured to be used onboard a Delta II 7925H launch vehicle with a payload fairing of 2.9 m and a payload fairing envelope of 2.54 m. This Delta 11 7925H launch vehicle is outfitted with a STAR-48B solid rocket motor developed by Alliant Techsystems. The adapter used for this three stage mission is the Boeing 3712A which has a mass of 45.4 kg and 0.94 m diameter. The Boeing 3712A adapter makes use of four matched spring actuators to reduce separation-induced tip-off rates. The adapter has two 37-pin spacecraft interface electrical connectors that are placed across the separation plane.

8.1.b. BUOI Probes

The Ballistic Unit and Operational Impactor (BUOI) probes allow for a more detailed look at the surface and internal characteristics of the asteroid Apophis. The probes, propelled by a thruster, impact the surface of the asteroid at up to 100 m/s while the main spacecraft records the effects and ejecta. The probes are launched near each other to determine the seismic activity created by the impact of the subsequent probes. Landing location are determined based on site conditions. This information aids the determination of the internal structure of the asteroid which may prove essential to future mitigation. A detailed time breakdown of the instrumentation can be seen in Figure 8-2. Most of the technology on the probes has previously been developed for the Deep Space 2 (DS2) mission, which lowers their overall risk and cost.

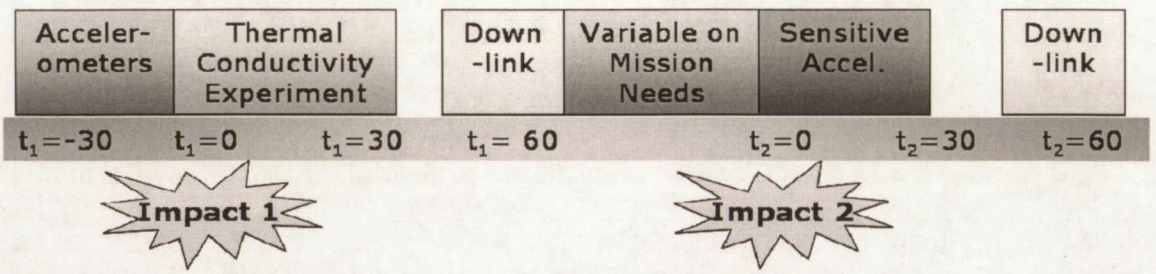

Figure 8-2. The operational timeline of the BUOI probes allows for the science objectives to be met while conserving power during non-use.

Structure

The BUOI Probe structure is modeled after the DS2 probes in order to ensure reliability. It can be broken down into three parts, the forebody, the aftbody, and a structural shell. (see Figure 8-3) The structural shell is used to lessen the effects of the impact as well as provide a mounting structure for a spin up mechanism. In addition to the DS2 structure, the probes will have reflective tape on their aftbody allowing the main spacecraft to locate them in order to determine their location better. Also, in future missions they can be easily found in order to act as reference points on the asteroid.

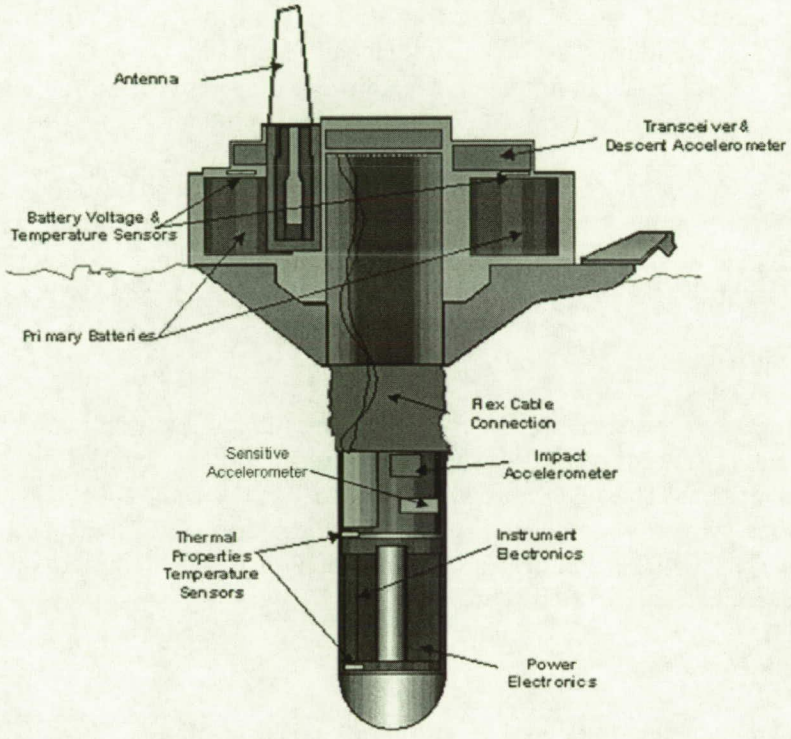

Figure 8-3. The structural integrity of the impactor shell protects the subsystems of the BUOI probe from the force of the impace with Apophis' surface.

Propulsion

A reliable cold gas thruster is used to propel the probes into the asteroid up at up to 100 m/s. A nitrogen cold gas thruster was chosen to create the velocity needed to impact the probes into the asteroid. If the impact is not fast enough, then the probes may not become properly embedded in the asteroid surface. Nitrogen was chosen since it is known that it is not present on Apophis. This fact is essential in obtaining proper composition analysis of the probe's ejecta. Once desired velocity is reached, the system separates and a small opening vents excess propellant in order to propel the system away from the landed BUOIs.

ADCS

Spin stabilization of the probes after detachment from the main spacecraft will ensure an accurate trajectory. The probes are pointed using the main spacecraft and then spin stabilized to a rate of 5 radians per second to ensure pointing. The stabilization is created by two nitrogen cold gas thrusters on either side acting as spinners.

Power

The BUOI Probes use reliable battery technology to increase their lifetime and therefore increase their mission importance rating. The power is provided by primary Lithium thionyl-chloride (Li-SOCl2) batteries. These batteries have been extensively tested on the DS2 mission and therefore cost less than they would be without testing. In addition, they provide more than adequate power for the entire mission lifetime.

A subsystem power breakdown can be seen in the Appendices. The batteries are capable of providing 104.4 W/hr of power even in cold conditions. Since our power constraints are less than those of the DS2, a similar battery package is chosen for the BUOI probes. This includes two sets of four cells each. With all systems constantly operational, the probe will last 45 hours.

Telecommunications

The telecommunications system previously flown on the DS2 mission allows for minimum testing while retaining reliability. It uses the Ultra High Frequency band (UHF) to communicate with the main spacecraft. This data is then relayed to Earth via the Deep Space Network. The telecommunications system is composed of a transponder and a 12.7 cm titanium antenna with 5.1 cm whiskers. The whiskers allow for the total length to be increased by the same length without an increase in structural shell size.

Command & Data Handling

The command and data handling system primarily consists of an Advanced Microcontroller (AMC). This small chip is capable of data collection, data storage, data transfer, and sequencing while using little power. It has been extensively tested at high impact velocities to ensure reliability. The AMC is preprogrammed before launch with the specific mission timeline to perform and is therefore autonomous from the main spacecraft and ground control.

Thermal

The instrumentation onboard the BUOI probes is designed to withstand the temperature ranges of Apophis with minimal thermal control. As seen in Table 8.2, the instrumentation is maintainable at wide temperature ranges. From a thermophysical model of Apophis, the temperature ranges are estimated to be 87 °C to -63 °C. For this reason, 15 layers of Multi-Layer Insulation is used to help protect the craft. Heat rejection occurs during periods of shadow due to the rotation of Apophis.

Table 8.2. All of the instruments onboard the BUOIs will be able to survive with minimal thermal control

*All In Celsius	Operational		Maintain	
	Low	High	Low	High
Instrumentation				
Temperature Sensor	-120	30	-150	50
Impact Accelerometer	-120	30	-150	50
Sensitive Accelerometer	0	70	-55	125
Descent Accelerometer	-80	30	-90	50
Subsystems				
AMC	-120	30	-150	50
Batteries	-80	25	-90	30
Telecom	-80	20	-90	50

Instrumentation

The instrumentation chosen for the BUOI Probes relies on heritage sensors to provide valuable data of the asteroid's surface and internal characteristics. The sensors include a temperature sensor as well as three different accelerometers. A mass and power breakdown of these systems can be seen in Table 8.3.

Table 8.3. The BUOI Probe instrumentation allows for low mass and power to increase efficiency

Instrument	Mass (g)	Peak Power (mW)
Temperature Sensors	2	55
Impact Accelerometer	0.75	250
Sensitive Accelerometer	0.75	3.5
Descent Accelerometer	1	65
Electronics	0.09	3.7
Subtotal	4.6	377
With Contingency	5.5	453

Temperature Sensors

Temperature sensors located in the forebody are effectively used to determine the conductivity of the soil. The impact of the probes transfers heat into the asteroid soil. For the first 30 minutes after the impact, two sensors separated by 20 cm continuously measure the temperature. As the temperature returns to equilibrium, the soil conductivity is determined. This information is useful in the determination of composition, cohesion, and the Yarkovsky effect.

Descent Accelerometer

A descent accelerometer is activated from the time of detachment to the time of impact. Located in the aftbody, this sensor helps to determine the final velocity from the cold gas thruster. It has a sample rate of 20 Hz, a resolution of 25 mg, and a range of +/- 50g.

Impact Accelerometer

An impact accelerometer is useful in the determination of surface characteristics of the asteroid. From the descent accelerometer, the theoretical depth of impact is determined. The variation from this depth aids in the determination of surface characteristics such as composition and cohesion. A one axis accelerometer is aligned with the z axis of the probe. This accelerometer has a maximum measuring range of 30,000g with a resolution of 10 mg.

Vibration Sensitive Accelerometer

A highly sensitive accelerometer is used to measure the vibrations from nearby probe impacts. The sensor is located in the forebody in order to record the maximum effect of the ground displacement. The ADXL 213 is a compact, low power dual-axis device that is highly sensitive to both static and dynamic accelerations. It has a range of +/- 1.2 g and a sensitivity of 1 mg. Its high sensitivity allows it to be able to measure small vibrations created from impacting probes nearby. This data is very useful in the determination of the internal structure of the asteroid. This information is important especially if future mitigation that involves impacting, drilling, or surface operations are needed.

8.2. Spacecraft Optimization

Ultimately, design selections were made and verified with the use of a global trade of all relevant switches and inputs into the Excel vehicle sizer. Discrete variables in this optimization were main propulsion system type (N_2H_4 monopropellant, N_2O_4/MMH bipropellant, N_2O_4/N_2H_4 bipropellant, and ion propulsion), RCS propulsion system type (N_2H_4 monopropellant and N_2O_4/MMH bipropellant), power system type (RTG, conventional solar arrays, and UltraFlex 175 solar arrays), and battery type (NiCd, NiH_2, and Li-Ion). Each combination of discrete variables (72 total combinations) was evaluated automatically within the Excel sizer to determine the vehicle with minimum boosted mass (and thus maximum launch margin and, most often, minimum cost). The total population of cases evaluated is shown in Figure 8-4 below, with the lowest-mass case (721.3 kg) being the dual-mode propellant system chosen (N_2O_4/N_2H_4 main propulsion with N_2H_4 RCS propulsion) with UltraFlex 175 solar arrays and lithium-ion batteries.

For each combination of discrete variables, antenna diameter was also automatically varied to minimize boosted mass. The significant variation of vehicle boosted mass with antenna diameter is shown in Figure 8-5. Note that while dozens of other variables exist within the sizer, none other were identified to have a meaningful mass-optimizing result. For example, while required data rate is an input into the sizer, the mass-optimum data rate is zero (or any pre-specified minimum).

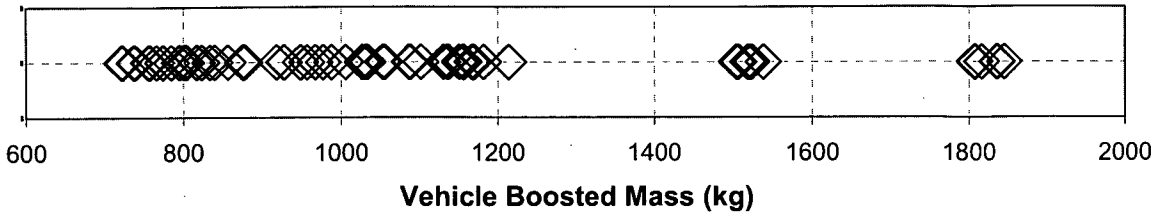

Figure 8-4. Of this population of 72 designs evaluated, the minimum-mass case is the chosen design for *Pharos*, with a mass of 721.3 kg.

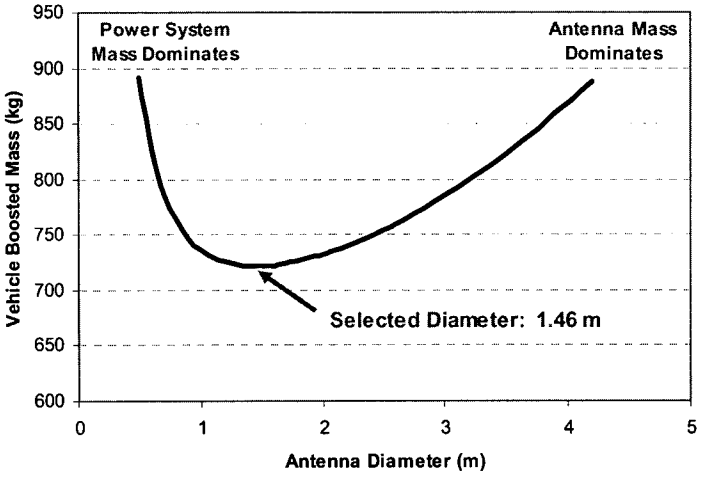

Figure 8-5. The variation of vehicle boosted mass with antenna mass is due to the trade between antenna mass and power system mass required to support necessary bitrates.

9. Mission Design

Cost-based constraints used mission data in order produce mission profile requirements for which spacecraft mass and program cost are significantly reduced. These constraints are the main drivers of the launch window and other phases.

9.1. Launch Phase

The determination of launch and arrival dates begin with the construction of pork chop plots showing Earth escape velocities for a large range of launch and arrival dates. The ephemeris data for Earth and Apophis is taken from the JPL's Horizons database and transferred into MATLAB via MS Excel spreadsheets. A Lambert Solver is then used to find the launch and arrival velocities for all relevant dates using the Universal Variable iteration scheme. The velocities are then changed from heliocentric velocities to body-centric escape velocities, resulting in the final pork chop plot. The velocity data from the entire mission timeline, from present day to end-of-life, is passed into the cost model developed as part of the systems

engineering methodology discussed earlier. Payload mass is assumed to be approximately 50 kg, allowing vehicle mass and cost to be estimated for a range of launch and arrival dates (i.e. for a variety of launch vehicle C3s and Apophis arrival ΔVs). Sample C3, ΔV, and cost pork-chop plots are shown in Figure 9-1.

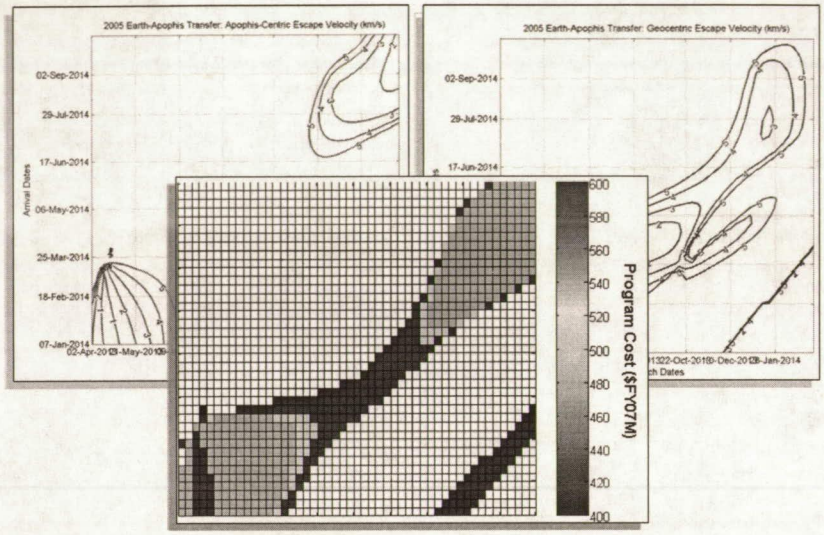

Figure 9-1. A sample set of C3 (upper right), ΔV (upper left), and cost (center bottom) pork-chop plots used to determine optimum launch date indicate a close correlation between cost and Apophis arrival ΔV (rather than launch vehicle C3).

Results show that near the minimum-cost launch window, program cost tends to be lowest when arrival ΔV at Apophis is lowest. An excerpt of a pork chop plot centered on the final launch window is shown below in Figure 9-2, and the relevant information concerning the launch window is listed in Table 9.1.

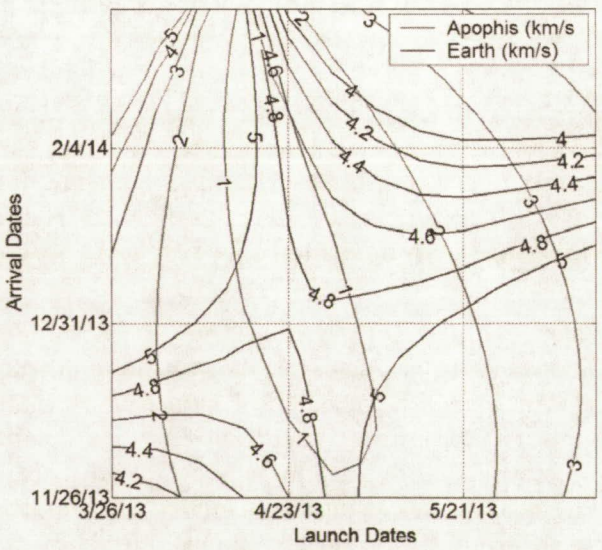

Figure 9-2. The chosen launch window is a result of determining what times during the mission satisfy to cost-based requirements.

Table 9.1. A high injection C3 is necessary to obtain the lowest possible arrival ΔV at Apophis.

Launch Dates	4/15/13 - 5/5/13
Arrival Dates	12/2/13 - 3/14/14
Injection C3 (km^2/s^2)	21.41 - 25.00
Arrival ΔV (km/s)	0.69 - 1.00

The Delta II 7925H is the chosen launch vehicle for *Pharos* because it is equipped to provide the needed C3 for a direct injection into a hyperbolic, Earth-escape trajectory and costs less than the next best choice, the Atlas V launch vehicle.

9.2. Cruise Phase

Seven days after leaving the gravitational influence of Earth, the spacecraft performs the first of four Trajectory Correction Maneuvers (TCMs), which requires 20 m/s of ΔV. This number was calculated by a 78,000-case Monte Carlo simulation using the injection ΔV tolerance as the uncertainty. This tolerance is calculated from a given Isp error from the Delta II 7925H Payload Planner's Guide and was assumed to be a 3σ error that has a normal distribution around the target injection velocity. Results of the Monte Carlo simulation are shown in Table 9.2.

Table 9.2. Margin added to a 3σ-confidence estimate ensures that TCM-1 is adequate to keep *Pharos* on target.

3σ ΔV (m/s)	16.48
Margin (m/s)	3.52
Total ΔV (m/s)	**20.00**

The remaining TCMs are based on historical TCM profiles of asteroid missions that examined how the subsequent TCMs were scaled down as percentages of the first TCM. These percentages were then applied to *Pharos*' first TCM to determine the remaining TCM budget and schedule. Details of the entire TCM budget are shown in Table 9.3. BLASST's estimate of the TCM ΔV allows a high-accuracy approach to *Pharos* at a small cost. and a detailed TCM schedule is shown in Figure 9-3.

Table 9.3. BLASST's estimate of the TCM ΔV allows a high-accuracy approach to *Pharos* at a small cost.

Maneuver	ΔV (m/s)
TCM-1	20.0
TCM-2	5.7
TCM-3	1.1
TCM-4	0.1
Total	**26.9**

9.3. Apophis Rendezvous Phase

The braking schedule of *Pharos* consists of three ΔV burns to remove the 690 - 1000 m/s of relative Apophis arrival velocity. Cowell's method is used to propagate the trajectory between each ΔV starting at a range of 150 km from Apophis and ending 1 km from Apophis. The model for which Cowell's method is used assumes that Apophis has a spherical gravity distribution and point mass, and that all other perturbers have negligible effect on the spacecraft during the short rendezvous phase. The first and second burns remove all but the final 1% of the escape velocity, and the third burn removes the residual velocity upon arrival at the 1000 m hover radius. Details of the braking schedule are shown in Table 9.4 and Figure 9-4.

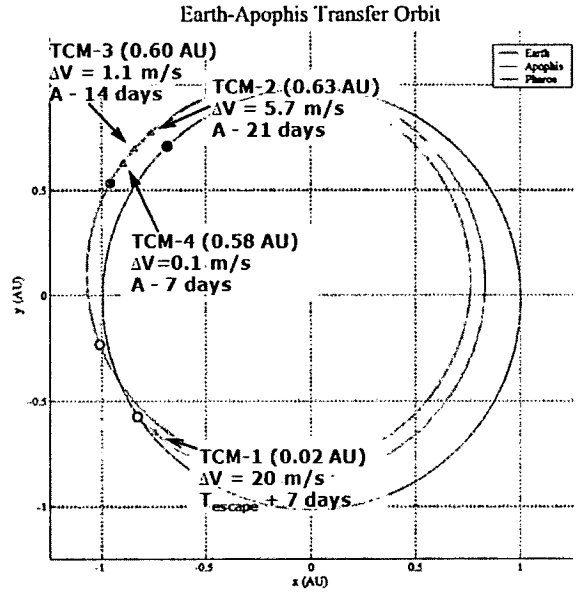

Figure 9-3. Four TCMs place *Pharos* on an accurate approach to Apophis.

Table 9.4. A slow arrival allows *Pharos* to come to a near stop in just under half an hour before it drifts to its operational distance.

Time (min)	ΔV (m/s)
A - 523	583.5 - 900
A - 503	106.8 - 99
A - 0	0.7 - 1

The uncertainty of the mass estimate of Apophis varies by a factor of three, which is the reason for the long freefall period before *Pharos* is brought to a complete stop in the vicinity of 1000 m. If the ΔV schedule took place when *Pharos* was closer to Apophis, *Pharos* would risk collision with Apophis instead of hovering near its surface. *Pharos*' stopping range will vary due to the uncertainty in Apophis' mass as see in Table 9.5.

Table 9.5. The uncertainty of the mass estimate of Apophis has very little effect on the ΔV schedule of *Pharos*.

Mass (kg)	Approach Speed	
	1 km/s	.69 km/s
	Hover Radius (m)	
7.00E+09	1018.9	1070.1
2.10E+10	1016.6	1066.1
6.30E+10	1009.6	1054.1

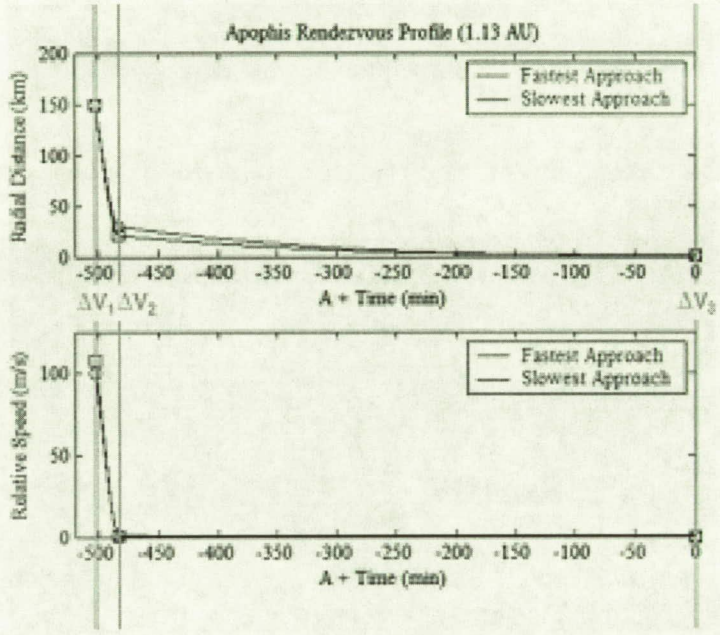

Figure 9-4. The timing of the ΔV burns allows for controlled and accurate placement of the *Pharos* spacecraft.

9.4. Proximity Operations

A SIMULINK model of *Pharos*' hover modes was run to determine the rate of fuel consumption at each of the hover radii. The final ΔV for maintenance was attained by budgeting for spending 100 weeks of the discretionary phase at the 500 m radius. A margin of 20 weeks is added in to account for uncertainty in the estimation of Apophis' mass. The results of the SIMULINK analysis are shown in Table 9.6. In this model, the mass of Apophis is assumed to be 2.1×1010 kg. The effect of uncertainty of Apophis' mass would change the fuel consumption rate by almost a factor of three, affecting the amount of time *Pharos* would be able to spend at the 500 m radius during the discretionary phase.

Table 9.6. The low mass of Apophis makes it possible to complete the 1000 m and 500 m Phases for less than 4 kg of fuel.

Hover Radius	Fuel Consumption (kg)		
	Per Day	Per Week	Per Month
500 m	0.1081	0.7567	3.243
1000 m	0.027	0.1194	0.8115

Based on conservative Apophis gravity and solar perturbation estimates, *Pharos* requires 460 m/s of ΔV to maintain its distance from Apophis over its lifetime.

As a disposal strategy, *Pharos* descends to the surface of Apophis rather than remaining adrift. Any fuel remaining in the RCS will be burned to slow the decent. The dates during which these phases occur are shown in Table 9.7.

Table 9.7. The short duration of the 1000 m and 500 m phases allows for a long discretionary phase.

Phase	Earliest Arrival	Latest Arrival
1000 m Phase	1/2/13 - 3/17/14	4/14/14 - 7/1/14
500 m Phase	3/17/14 - 4/17/14	7/1/14 - 8/1/14
Discretionary Phase	4/17/14 - 12/31/16	8/1/14 - 12/31/16

9.5. Apophis Orbit Determination

Pharos builds on previous missions to asteroids and comets in the solar system. An important difference between *Pharos* and all others is in the emplacement of navigational assets at Apophis such that precise orbit determination can be accomplished by 2016.

With the trajectory predicted to pass closer than geostationary orbit on Apophis' 2029 flyby, there is likelihood that perturbations could cause the asteroid to impact Earth on its subsequent 2036 flyby. Specifically, the 2029 passage of Apophis must not pass through a 610 m region denoted as the 2036 keyhole as seen in Figure 9-5. If the keyhole is breached, the asteroid will hit Earth on its subsequent return in 2036. By precise orbit determination techniques, *Pharos*' primary mission objective is to specify within 0.126-σ (10% confidence) bounds that the true Apophis orbit will not hit the 2036 keyhole during its passage in 2029. This precise orbit determination data is returned to the *Pharos* science team for analysis, completed before the 2016 deadline.

The precise orbit determination desired for *Pharos* requires a communications system on a spacecraft at Apophis. Via NASA's Deep Space Network (DSN), the position and velocity of a spacecraft is determined using Tracking Data Type (TRK). This involves two types of measurements, a ranging pulse determining position and the Doppler shift in the signal determining angular velocity. The accuracy of position and velocity determined using the DSN results in 1 m and 1 mm/s uncertainties, respectively.

Analysis of 100 potential true Apophis trajectories via 15-body solar system orbit propagation and Kalman filtering indicates, as shown in Figure 9-5, that a weekly DSN ranging plan results in no 10% confidence ellipses breaching the 2036 keyhole. If it is assumed that integration errors in BLASST's orbit propagator result in a worst-case scenario with the center of the keyhole at the center of the true orbit probability distribution, it is found that only 1% of potential true Apophis orbits intersect the keyhole. A sample 10% confidence error ellipse is shown in comparison to the 2036 keyhole in Figure 9-5.

Thus, *Pharos* will take 146 measurements over 146 weeks to demonstrate that 99% of possible true Apophis orbits will not hit the 2036 keyhole within 10% confidence.

Also included in the category of precise orbit determination are physical characteristics of Apophis such as composition and mass properties. The combination of state vector, rotation rate, composition, and mass properties all allow for the analysis of the Yarkovsky Effect. The rotating body absorbs heat during its daytime and re-radiates the heat in a direction during its nighttime. This re-radiation of energy causes uncertainties in the state vector and therefore trajectory predictions. Increased knowledge of the Yarkovsky Effect during the mission duration will lead to a more accurate state noise characterization and orbit error propagation.

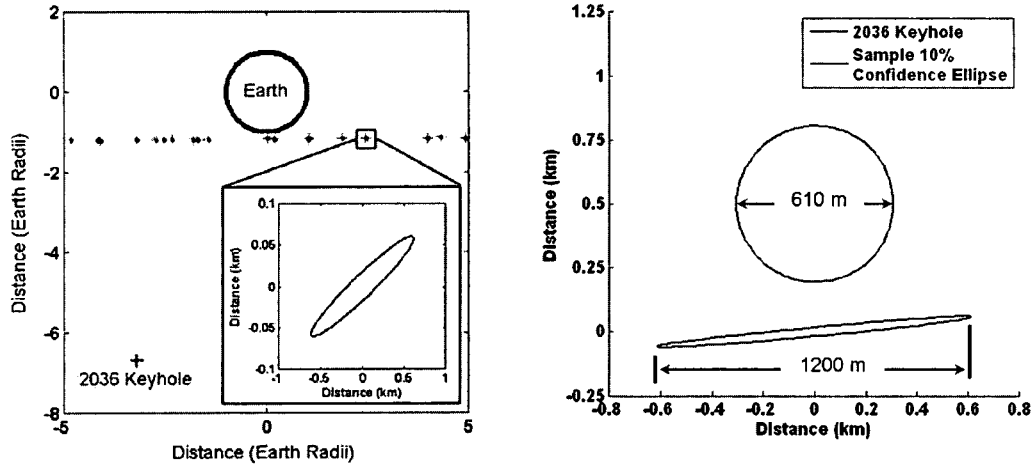

Figure 9-5. The keyhole and the propagated error ellipses for each of the 100 cases are both projected on Earth's b-plane.

10.Project Management

10.1. Organization

BLASST Space Systems is a small aerospace group located in Atlanta, Georgia. Our team has in-depth experience with spacecraft design and systems engineering. The team representing BLASST Space Systems is in Figure 10-1. The responsibilities of each member are as follows:

- The ***Project Manager***, Jonathan Sharma, heads the organizational and presentation aspects of the team and acts as the functional team leader.
- The ***Lead Systems Engineer***, Jarret Lafleur, is primarily responsible for ensuring a systematic and comprehensive downselection process and for managing programmatic margins and integrating individual mass, power, and volume models into master vehicle models.
- The ***Lead Spacecraft Systems Engineer***, Kreston Barron, is responsible for subsystem design of individual subsystem mass, power, and volume models.
- The ***Lead Mission Systems Engineer***, Jonathan Townley, leads the implementation of orbital mission design, mission timelines, launch vehicle trades, and operations plan development.
- The ***Orbit Determination Payload Specialist***, Nilesh Shah, is responsible for the investigation of Apophis orbital determination requirements and implementation.
- The ***Science Payload Specialist***, Jillian Apa, is responsible for the development of the requirements and implementation plan for the investigation of Apophis in terms of scientific objectives.

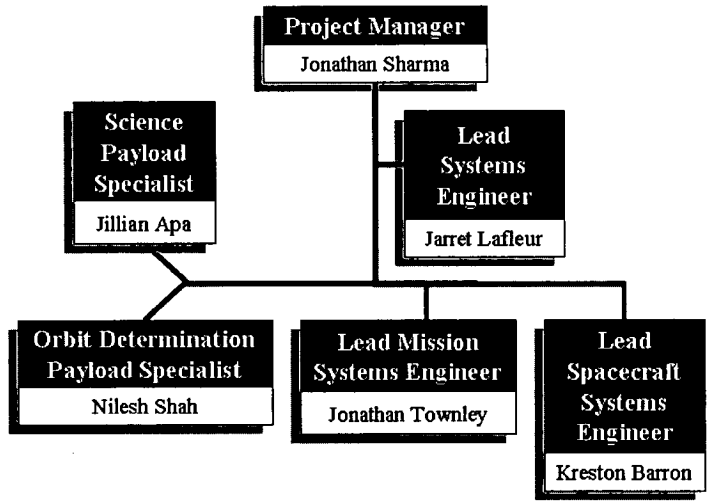

Figure 10-1. BLASST Space Systems consists of highly qualified individuals in their respective fields.

10.2. Schedule

Pharos is completed with generous margins as seen in Figure 10-2. The critical path in red follows the mission definition through a portion of preliminary design. Development of the BUOIs begins in Phase B because they require over two years of development time and are a key factor in *Pharos*. The schedule is flexible by allowing margins along all paths. These margins depend on the overall time spent on each item. The critical schedule margin amounts to almost one year.

The phase lengths are determined based off AO requirements and historical models where applicable. Step-1 proposals are due by April 25, 2007. The Phase A Concept Study Report is due in October 2008. Phase C/D lasts no longer then 52 weeks. There are no limits on Phase B or E. December 31, 2016 is the date of mission completion

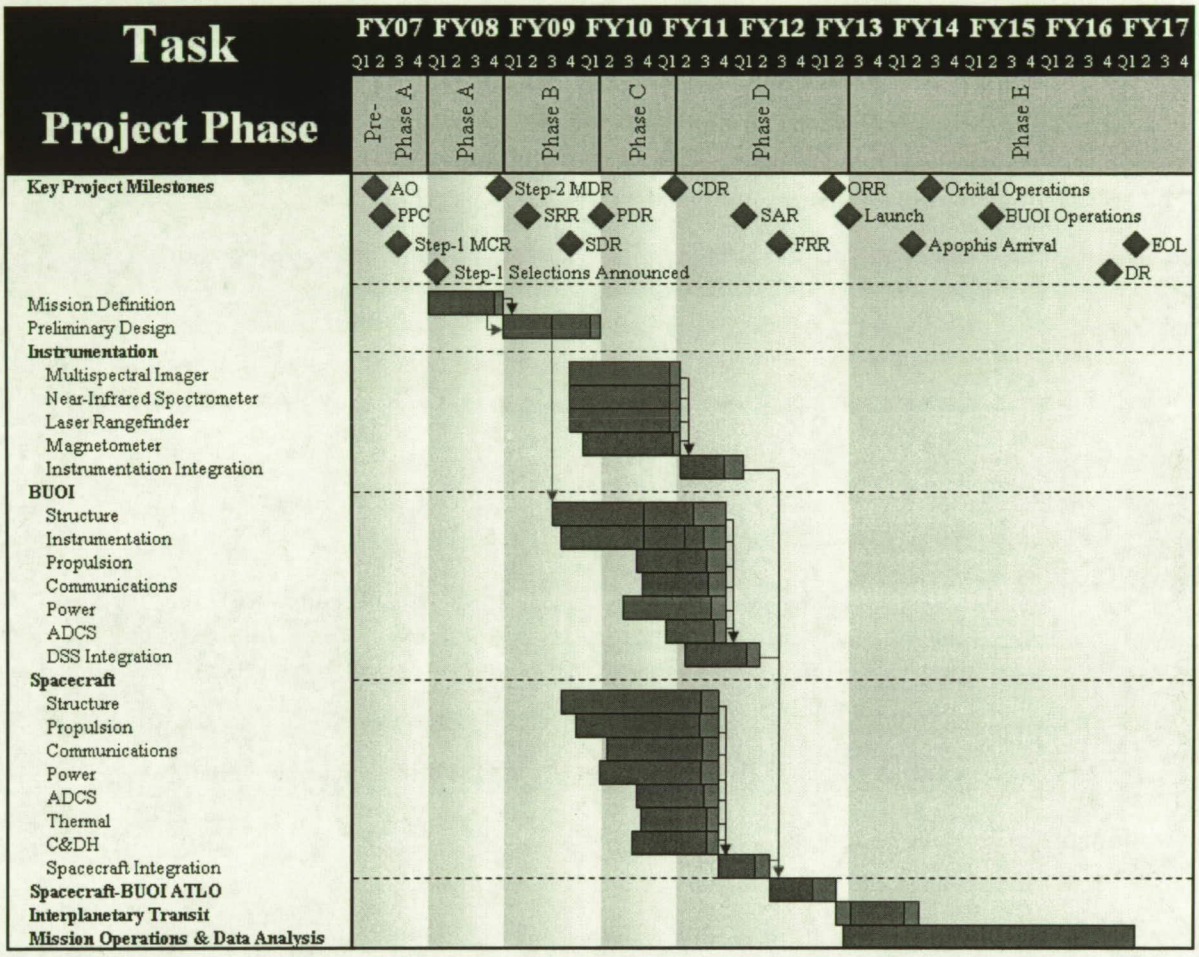

Figure 10-2. The BUOI probes involve the majority of the critical path (red) allotting for a high level of development in that area.

10.3. Redundancy and Reliability

The *Pharos* mission and spacecraft design team has integrated redundancy and reliability analysis and design decisions to ensure the greatest probability of mission success at a reasonable cost to NASA. Analyses include a Functional Hazard Assessment (FHA) of mission phases, reliability block diagrams (RBDs) to represent redundancies associated with the achievement of mission objectives, and trade studies to assess subsystem redundancy options.

The FHA shown in Table 10.1 identifies major failure modes at different stages of the *Pharos* mission. A classification of "Catastrophic" is used to indicate a scenario leading to the destruction or loss of a functional vehicle. The term "Major" is used to describe a scenario resulting in at least a partial loss of mission, and "Minor" entails functional degradation of spacecraft or mission performance. "No Capability Effect" designates a scenario resulting in zero or negligible performance degradation.

This FHA leads the design team to several subsystem design decisions to ensure mission success. Highlights include:

- Inclusion of two main engines, each canted slightly to thrust through the vehicle center of mass and each capable of a fully-loaded thrust-to-weight of 0.07.
- Use of simple and reliable hypergolic propellants (N2O4 and N2H4), including common RCS and main fuels.
- Use of 50% redundant solar arrays, given the consequences of a solar array power failure. UltraFlex 175's advanced array technology allows a 63% array mass reduction, even with 50% redundancy.
- Inclusion of a small navigation camera within ADCS to allow redundancy for visual ranging to Apophis during approach and insertion phases.
- Inclusion of an auxiliary low and medium-gain antennas to allow emergency commanding in the event of a temporary main antenna failure. Data rates are sufficient to maintain a minimum level of science from the NLR, NIS, MAG, and BUOIs in the event of a main antenna failure early in the mission.
- Coverage to ensure near-real-time support during critical mission events.

Additionally, RBDs were constructed to track redundancy in the performance of objectives in Table 5.2. Key observations include:

- No single instrument failure will cause the loss of all eight mission objectives.
- No objective will completely fail as a result of a single instrument failure.
- Goals related to impactor probe performance are especially robust to failure since four probes are carried aboard *Pharos*. The greatest concern for the probes, impact survival, is mitigated by the ability of probes to control ΔV imparted by the main thruster if previous launches fail.
- Given a functioning communications system, complete failure of state vector determination (Priority #1) will occur only if the NLR, MSI, BUOI probes, and navigation camera fail.
- Complete failure of the re-radiation dynamics objective will only occur if the BUOI probes, NLR, MSI, NIS, and navigation camera fail.

Table 10.1. This Functional Hazard Assessment (FHA) of the *Pharos* mission identifies the reliability considerations which factored into key vehicle and mission design decisions.

Mission Phase	Function	Failure Condition	Effect	Classification
Launch	Ascent	Lift-off Failure: Scrub prior to ignition	Launch rescheduled to next window.	No Capability Effect
Launch	Ascent	Launch Vehicle Failure to achieve orbit	Vehicle burns up on return to Earth.	Catastrophic
Launch	Injection	Launch Vehicle Failure to inject into proper hyperbolic orbit	Vehicle unable to achieve original mission.	Major, unless vehicle able to make up ΔV deficit to perform an altered mission.
Deep Space Cruise	Trajectory Modification	Mid-course Burn Failure	Vehicle may miss asteroid target.	Minor, if recovered in future correction burns
Deep Space Cruise	Trajectory Modification	Subsystem Checkout Failure	Vehicle not cleared for original mission.	Major, if problem unresolvable and future checkouts fail.
Deep Space Cruise	Trajectory Modification	Navigation Camera Failure	State of approaching asteroid unknown.	Minor, if MSI available.
Apophis Arrival	Insertion & Approach	Single Engine Ignition Failure	Switch to backup engine (or RCS if final approach).	Minor, if backup engine (or RCS if final approach) okay.
Apophis Arrival	Insertion & Approach	Pointing Failure	Residual asteroid-relative velocities exist.	Minor, if residual velocities are within tolerable limits.
Apophis Arrival	Insertion & Approach	Navigation Camera Failure	State of approaching asteroid unknown.	Minor, if MSI available.
Apophis Operations	High-Orbit, Close-Look Orbit Modes	Maintenance RCS Failure	Vehicle at risk for uncontrolled impact within approx. 3-4 hrs.	Minor, if detected and corrected by unused RCS thrusters.
Apophis Operations	Probe Launch	Probe Release Failure	Probe unable to deploy to impact target.	Major, unless deploy mechanism repairable.
Apophis Operations	Probe Launch	Spinup Failure	Probe may not impact at correct target or attitude.	Major
Apophis Operations	Probe Launch	Main Thruster Failure	Probe will not impact target at correct velocity.	Minor, if thruster underburns.
Apophis Operations	Probe Launch	Pointing Failure	Probe will not impact at correct target or attitude.	Major
Apophis Operations	Probe Launch	Instrument Initialization Failure	Impact data not recorded.	Major (only ejecta analysis possible)
Apophis Operations	Probe Launch	Impact Failure	Probe destroyed, damaged, or fails to lodge.	Major (only ejecta analysis possible)
Apophis Operations	Probe Operations	Probe Subsystem or Instrumentation Failure	Premature probe mission termination.	Major
End of Life Disposal	Landing	Loss of Vehicle due to Hard Landing, Subsystem or Pointing Failures	Termination of mission and elimination of potential for mission extension.	No Capability Effect (end of mission)
End of Life Disposal	Power-Down	Failure to Power Down	Potential for vehicle re-contact eliminated.	No Capability Effect (end of mission)
All		Complete Solar Array Failure	Loss of vehicle within approx. 2 hrs.	Catastrophic, if arrays not restored.
All		Antenna Gimbal Failure	ADCS or RCS required for antenna pointing.	Minor
All		Main Antenna Failure	Vehicle switches to backup quad helix antenna for emergency commanding.	Major, if main antenna cannot be restored.
All		ADCS Failure	RCS required for pointing.	Major, if ADCS not restorable.
All		Debris Impact	Subsystem or instrument damage.	Catastrophic, if impact energy high enough.
All		Instrument Failure	Dependent on instrument (see discussion).	Major, but no one instrument fails all science objectives.

10.4. Risk

While BLASST Space Systems classifies *Pharos* as a low-risk mission, its design and implementation plan includes several risk-mitigating programmatic and management features. *Pharos* is designed with generous margins and contingencies on schedule, cost, power, and mass. Substantial use of heritage instruments from previous exploration missions reduces the already-small likelihood that these margins will be breached.

Additionally, BLASST will designate a safety and mission assurance (S&MA) manager and an S&MA team upon entrance into Phase B to oversee risk management through end of life. This team coordinates closely with the NASA Headquarters Office of Safety and Mission Assurance (OSMA) to ensure adherence to standard NASA risk guidelines. A Probabilistic Risk Assessment (PRA) for this mission is not required.

10.5. Descope

BLASST mitigates uncertainty in mission cost, schedule, mass, and power by grounding the *Pharos* proposal in heritage technologies, applying generous budget margins, and utilizing science instruments which each fulfill several objectives. In the event that these efforts are insufficient, five descope options are defined to reduce mission capabilities but still allow an acceptable cadre of science activities.

Table 10.2 details these descope options, including launch mass, power, and cost savings if the options are implemented prior to the beginning of Phase C. The ultimate deadline for each decision is also listed, as are associated impacts on the science mission.

Table 10.2. The *Pharos* mission reserves five descope options which reduce mission capabilities but still allow an acceptable cadre of science activities.

Descope Option	ΔLaunch Mass (kg)*	ΔPower (W)*	ΔCost (FY07$M)*	Science Impact	Decision Deadline
Delete MAG	-6.6	-3.7	-0.6	Magnetic field presence unmeasurable.	Instrumentation Integration (2011)
Delete 2 BUOI probes	-35.8	0.0	-1.1	50% reduction in Probability of success for probe objectives.	BUOI Integration (2011)
Eliminate solar array redundancy	-28.9	0.0	-14.1	33% increase in risk of power failure.	Spacecraft Integration (2011)
Reduce onboard RCS propellant by 50%	-79.1	0.0	-1.0	Reduce operational lifetime by 1 year.	Launch (2013)
Reduce science data collection by 80%	-34.0	-100.4	-10.7	Reduce data capacity to 10 MSI-class images per day.	End of Life (2016)

**If descoped prior to start of Phase C*

10.6. Cost

10.6.a. Cost Estimation Methodology

Several cost estimating tools are used in *Pharos*. Major costing is done in three stages: initial estimation, validation, and refinement. Costing of the spacecraft and mission operations is done with WeLCCM98. Developed by Georgia Institute of Technology's Space Systems Design Lab, it estimates the life cycle cost for NASA Discovery type missions. This provides the majority of costs. The spacecraft costs are verified using parametric techniques outlined in Space Mission Analysis and Design based off historical small satellite data. Mission operations cost data is verified using Johnson Space Center's Mission Operations Cost Model which is based on historical NASA data. Cost spreading is done by using either beta curves or averaging the FY07 cost over the time span.

The documentation provided in NASA's Mission Operations and Communications Services is used to determine the cost of using the DSN based off hours of usage. These hours are derived from data rates and communication subsystem sizing.

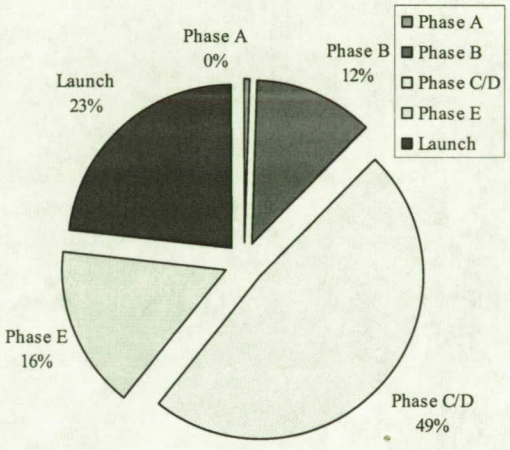

Figure 10-3. Costs are greatest during Phase C/D.

Instruments are sized using the Spacecraft/Vehicle Level Cost Model (SVLCM). SVLCM provides rough-order-of-magnitude cost estimation of development and production costs. The BUOIs utilize the production aspect of SVLCM and the historical analog cost of development of the Mars Microprobes they are based on.

The costs seen in each phase and launch of *Pharos* are seen in Figure 10-3. During each phase, the budget reserve is 30%.

10.6.b. Project Cost Estimate

Pharos is a low cost NASA mission well under the $500 million (FY07) cost cap. The total mission cost is $429.5 million (FY07). This includes a 30% reserve of $75.7 million (FY07). The cost is spread through the nine year mission timeline as seen in Figure 10-4. There are several instances in which costs go over the allotted cost cap. By using roll over from previous years *Pharos* manages to meet AO requirements. The full cost breakdowns are seen in the Appendices.

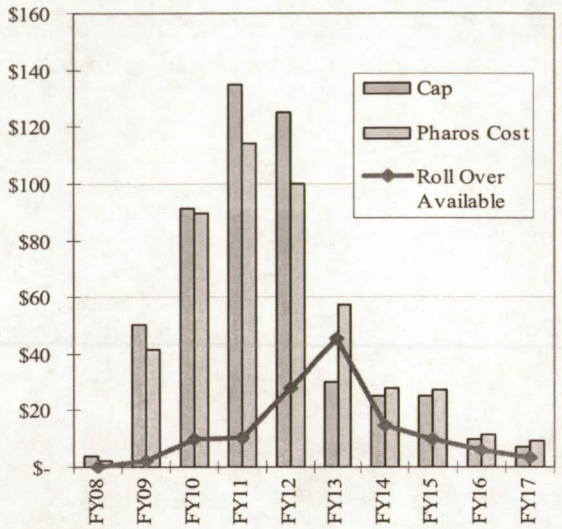

Figure 10-4. By utilizing rollover available from previous years, *Pharos* manages to stay on budget while going over the allotted cost cap.

11.Bibliography

- "99942 Apophis (2004 MN4) Earth Impact Risk Summary." NASA JPL Near Earth Object Program. 19 Oct. 2006. <http://neo.jpl.nasa.gov/risk/a99942.html> [27 March 2007].
- *ADXL213*. Norwood, MA: Analog Devices, 2004.
- *ADXL250*. Norwood, MA: Analog Devices, 1998.
- "Asteroid 99942 Apophis (2004 MN4)." *NASA Jet Propulsion Laboratory.* <http://neo.jpl.nasa.gov/cgi-bin/db?name=99942> [Accessed 29 March 2007].
- "Atlas Launch System Mission Planner's Guide Atlas V Addendum." *Lockhead Martin.* 1999. <http://www-eng.lbl.gov/~lafever/SNAP/Snap_17/Atlas%20V%20Payload%20Planners%20Guide.pdf >. [Accessed 29 March 2007]
- "ATK- Mission Systems." <http://www.atk.com/customer_solutions_missionsystems/cs_ms_space_sasps.asp>. [Accessed 29 march 2007]
- Behrend, R., comp. "Asteroids and Comets Rotation Curves and Regular Variable Stars Light Curves". *Observatoire de Genève.* <http://obswww.unige.ch/~behrend/page5cou.html>.[Accessed 29 Mar. 2007]
- Binzell, R. Personal Correspondence
- Cellinoi, A. et al. "Albedo and Size Determination of (99942) Apophis from Polarimetric Observations." *IAU Symposium* 236, 2006
- Chesley, S.R., "Potential impact detection for Near-Earth asteroids: the case of 99942 Apophis (2004 MN4)." Proceedings of IAU Symposium No. 229, Rio De Janeiro, 7-12 Aug. 2005.
- Cleave, M. L. NASA Science Mission Directorate. Letter to B612 Foundation Chairman Russell Schweickart. 12 Oct. 2005. <http://www.b612foundation.org/papers/Cleave_ltr.pdf > [Accessed: 28 March 2007].
- Cole, T. D. "NEAR Laser Rangefinder: a Tool for the Mapping and Topologic Study of Asteroid 433 Eros." *Johns Hopkins APL Technical Digest* 19, 1998.
- David, L. "NASA Studies Manned Asteroid Mission." Space.com. 16 Nov. 2006. <http://www.space.com/news/061116_asteroid_nasa.html >[Accessed 28 March 2007].
- "Delta Payload Planners Guides." *Boeing.* <http://www.boeing.com/defense-space/space/delta/guides.htm>. [Accessed 29 March 2007]

- Farquhar, R W., D W. Dunham, and J V. McAdams. "NEAR Mission Overview and Trajectory Design". *John Hopkins University Applied Physics Laboratory*. Laurel, MD, 1995.
- Hawkins, E. "The NEAR Multispectral Imager." *Johns Hopkins APL Technical Digest* 19, 1998.
- Holsapple, K A. "Crater Sizes for Explosions or Impacts." University of Washington. <http://keith.aa.washington.edu/craterdata/scaling/index.htm>. [Accessed 22 Apr. 2007]
- JPL Special Review Board. *Mars Polar Lander/Deep Space 2 Loss*. JPL D-18709 NASA Jet Propulsion Laboratory. Pasadena, CA, 2000.
- Larson, W. J., and J. R. Wertz, eds. *Space Mission Analysis and Design*. 3rd ed. El Segundo, CA: Microcosm P, 1999.
- Lewis, K., comp. *New Millennium Mars Microprobe Spacecraft Design*. NASA Jet Propulsion Laboratory. JPL D-14222, 1999.
- Lohr, D. A., L. J. Zanetti, B. J. Anderson, T. A. Potemra, and M. H. Acuna. "The NEAR Magnetic Field Instrument." *Johns_Hopkins APL Technical Digest* 19, 1998.
- Lorenz, R D., J E. Moersch, J A. Stone, A R. Morgan, and S E. Smrekar. "Penetration Tests on the DS-2 Mars Microprobes." *Planetary and Space Science* 48 (2000): 419-436.
- Melosh, H J., and R A. Beyer. "Crater." University of Arizona. <http://www.lpl.arizona.edu/tekton/crater.html>. [Accessed 22 Apr. 2007]
- NASA Planetary Protection website. 21 Nov. 2006. <http://planetaryprotection.nasa.gov/pp/> [Accessed 28 March 2007].
- NPR 8020.12C: Planetary Protection Provisions for Robotic Extraterrestrial Missions. 27 April 2005. <http://nodis3.gsfc.nasa.gov/npg_img/N_PR_8020_012C_/N_PR_8020_012C_.pdf>[Accessed 28 March 2007].
- Peacock, K., J. W. Warren, and E. H. Darlington. "The Near-Infrared Spectrometer." *Johns_Hopkins APL Technical Digest* 19, 1998.
- Reidel, J E., S Bhaskaran, S Desai, D Hand, B Kennedy, T McElrath, and M Ryne. "Autonomous Optical Navigation (AutoNav) DS1 Technology Validation Report". *NASA Jet Propulsion Laboratory*. Pasadena, CA, 2000.
- Sanii, B, and D. Jackson. "Near Earth Optical Acquisition and Communication Exploration". *Office of Contracts and Grants*. Report 2000-02. 2000.

- Schweickart, R. L. B612 Foundation. Letter to NASA Administrator Michael Griffin. 6 June 2005. <http://www.b612foundation.org/papers/Griffin_ltr.doc> [Accessed 28 March 2007].

- Sheeres, D J., L M. Benner, S J. Ostro, A Rossi, F Marzari, and P Washabaugh. "Abrupt Alteration of the Spin State of Asteroid 99942." *Icarus* 178. 281-283, 2005.

- Smrekar, S. "Deep Space 2: the Mars Microprobe Mission." *Journal of Geophysical Research,* 104. 27,013-27,030, 1999.

- "Solar System Exploration." 2006 Solar System Exploration Roadmap. NASA Science Mission Directorate. Sept. 2006. <http://solarsystem.nasa.gov/multimedia/downloads/SSE_RoadMap_2006_Report_FC-A_med.pdf> [Accessed 28 March 2007].

- Spence, B, S White, N Wilder, T Gregory, M Douglas, and R Takeda. "Next Generation UltraFlex Solar Array for NASA'S New Millennium Program Space Technology 8". *AEC-Able Engineering*. Goleta, CA.

- "U.N. urged to take action on asteroid threat." CNN.com. 19 Feb. 2007. <http://www.cnn.com/2007/TECH/space/02/19/asteroid.deflector.reut/> [Accessed 19 Feb. 2007].

- Ward, S.N. "2004MN4 Impact Tsunami Simulation." University of California Santa Cruz. <http://es.ucsc.edu/~ward/2004MN4(b).mov>[Accessed 27 March 2007].

12.Appendices

Pharos Mass Breakdown

WBS Designator	Item	CBE (kg)	Contingency	CBE + Contingency	Total (kg)
1.0	**Payload**				**62.4**
1.1.	MSI	9.6	10%	10.5	
1.3.	NLR	5.0	10%	5.5	
1.3.1.	MAG	1.5	10%	1.7	
1.3.2.	NIS	15.2	10%	16.7	
1.3.3	BOUIs (4)	28.0	(In BOUI WBS)	28.0	
2.0	**Spacecraft Subsystems**				**319.4**
2.1.	Propulsion				65.5
2.1.1.	Thrusters and Engines	12.0	10%	13.2	
2.1.2.	Fuel Tank (2)	6.2	15%	7.1	
2.1.3.	Oxidizer Tank (2)	3.1	15%	3.6	
2.1.4.	Helium Pressurant Tanks (4)	28.7	15%	32.9	
2.1.5.	Helium Pressurant	2.3	15%	2.6	
2.1.6.	Pressure Lines, Fittings, Valves, etc.	5.0	20%	6.0	
2.2.	Attitude Control				36.1
2.2.1.	Momentum Wheels (4)	18.4	20%	22.1	
2.2.2.	Star Sensor	2.7	10%	3.0	
2.2.3.	Sun Sensors (5)	1.9	10%	2.1	
2.2.4.	IMU	5.3	10%	5.8	
2.2.5.	Navigation Camera	2.7	15%	3.1	
2.3.	Communications				30.7
2.3.1.	Parabolic Ka-band Antenna	8.0	20%	9.6	
2.3.2.	Amplifiers and Transponders (2)	12.3	15%	14.1	
2.3.3.	Command Detector Units (2)	0.7	15%	0.8	
2.3.4.	Telemetry Conditioning Units (2)	1.7	15%	2.0	
2.3.5.	RF Switches, Coaxial Cables	3.0	15%	3.5	
2.3.6.	Auxiliary Antenna	0.7	15%	0.8	
2.4.	Command & Data Handling	12.5	20%	15.0	15.0
2.5.	Thermal				18.7
2.5.1.	MLI Blankets	15.0	20%	18.0	
2.5.2.	Heat Pipes	0.2	20%	0.3	
2.5.3.	TCS Electronics	0.2	20%	0.2	
2.5.4.	Heaters	0.2	20%	0.2	
2.6.	Power				61.9
2.6.1.	UltraFlex Solar Arrays (4)	4.5	20%	5.4	
2.6.2.	Lithium Ion Batteries	5.1	15%	5.9	
2.6.3.	Power Control Unit	13.9	20%	16.7	
2.6.4.	Regulators & Converters	17.4	20%	20.9	
2.6.5.	Wiring	10.9	20%	13.1	
2.7.	Structure & Mechanisms	76.2	20%	91.5	91.5
	Spacecraft Dry Mass	(330.0)	(16%)		381.8
3.0	**Propellant**				**294.1**
	Loaded Mass				675.9
4.0	**Adapter**				**45.4**
	Satellite Boosted Mass				**721.3**
	Total Margin				198.2
	Margin Percentage				27%
	Launch Capability of LV				**919.5**

Pharos Nominal Power Mode

CBE (W)	Contin.	CBE + Contin.	Total (W)
			45.1
8.3	5%	8.7	
16.5	10%	18.2	
1.5	10%	1.7	
15.1	10%	16.6	
0.0	10%	0.0	
			377.1
			5.5
5.0	10%	5.5	
0.0	15%	0.0	
0.0	15%	0.0	
0.0	15%	0.0	
0.0	15%	0.0	
0.0	15%	0.0	
			75.4
30.0	20%	36.0	
9.9	10%	10.9	
0.3	10%	0.3	
21.4	10%	23.5	
4.0	15%	4.6	
			51.9
0.0	0%	0.0	
47.6	0%	47.6	
3.8	15%	4.4	
0.0	15%	0.0	
0	0%	0.0	
0	0%	0.0	
25.0	20%	30.0	30.0
			9.2
0.0	15%	0.0	
0.0	15%	0.0	
3.0	15%	3.5	
5.0	15%	5.8	
			205.1
5.0	15%	5.8	
9.8	15%	11.2	
0.0	15%	0.0	
139.2	15%	160.1	
24.4	15%	28.0	
0.0	20%	0.0	0.0
Spacecraft Day Power			422.3
Total Margin			211.1
Margin Percentage			50%
Total Power Available			**633.4**

Pharos Shadow Power Mode

CBE (W)	Contin.	CBE + Contin.	Total (W)
			1.7
0.0	5%	0.0	
0.0	10%	0.0	
1.5	10%	1.7	0.0
0.0	10%	0.0	
0.0	10%	0.0	
			166.4
			0.0
0.0	10%	0.0	
0.0	15%	0.0	
0.0	15%	0.0	
0.0	15%	0.0	
0.0	15%	0.0	
0.0	15%	0.0	
			70.4
30.0	20%	36.0	
9.9	10%	10.9	
0.0	10%	0.0	
21.4	10%	23.5	
0.0	15%	0.0	
			0.0
0.0	0%	0.0	
0.0	0%	0.0	
0.0	0%	0.0	
0.0	0%	0.0	
0.0	0%	0.0	
0.0	0%	0.0	
25.0	20%	30.0	30.0
			9.2
0.0	15%	0.0	
0.0	15%	0.0	
3.0	15%	3.5	
5.0	15%	5.8	
			56.8
0.0	15%	0.0	
0.0	15%	0.0	
0.0	15%	0.0	
42.0	15%	48.3	
7.4	15%	8.5	
0.0	20%	0.0	0.0
Spacecraft Night Power			168.1
Total Margin			42.0
Margin Percentage			20%
Total Power Available			**210.1**

BUOI Probe Mass Breakdown

WBS Designator	Item	Mass (g)	Contin.	CBE + Contin. (g)
1.0	Communications	**25.6**	15%	**29.5**
1.1	Antenna	0.64		
1.2	Electronics	25		
1.2.1	Electronics (transmitted)			
1.2.2	Electronics (received)			
2.0	Power	**360**	10%	**396**
2.1	Batteries	360		
2.2	Wiring			
3.0	C&DH	**1**	10%	**1.1**
3.1	AMC	1		
4.0	Payload	**14.5**	20%	**17.4**
4.1	Temp. Sensor (2)	2		
4.2	Impact Accel. (2)	0.75		
	Sensitive Accel.	0.75		
4.3	Descent Accel.	1		
4.4	Electronics	10		
5.0	Structure	**3715**	20%	**4458**
5.1	Aftbody	1700		
5.2	Forbody	850		
5.3	Penetrator Shell	1165		
5.4	Added Weight		30%	**400**
6.0	Propulsion	**1307**		**1699.1**
6.1	Spinner (2)	178		
6.2	Thruster	1129		
Total		5423		7001.55
Total		**5.42 kg**		**7.0 kg**

BUOI Probe Power Modes

Operational (mW)		Maintain (mW)		Operational (mW)	Maintain (mW)
	1842.5		**55.0**	**2026.8**	**63.3**
0		0			
1842.5		55.0			
770.0		0.0			
	22.9		**0.56**	**0.0**	**0.67**
0		0.0			
23		0.56			
	50.0		**0.6**	**0.0**	**0.69**
50.0		0.6			
	377.2		**0.0**	**452.7**	**5.0**
55.0		0			
250.0		0			
3.5					
65.0		0			
3.7		0			
	0		**0**	**0**	**0**
0		0			
0		0			
0		0			
0		0			
	0.2		**0**	**0.24**	**0**
0.1		0			
0.1		0			
Total (mW	2292.66		56.16	2564.68	69.61
Total (W)	2.29		0.06	2.56	0.07

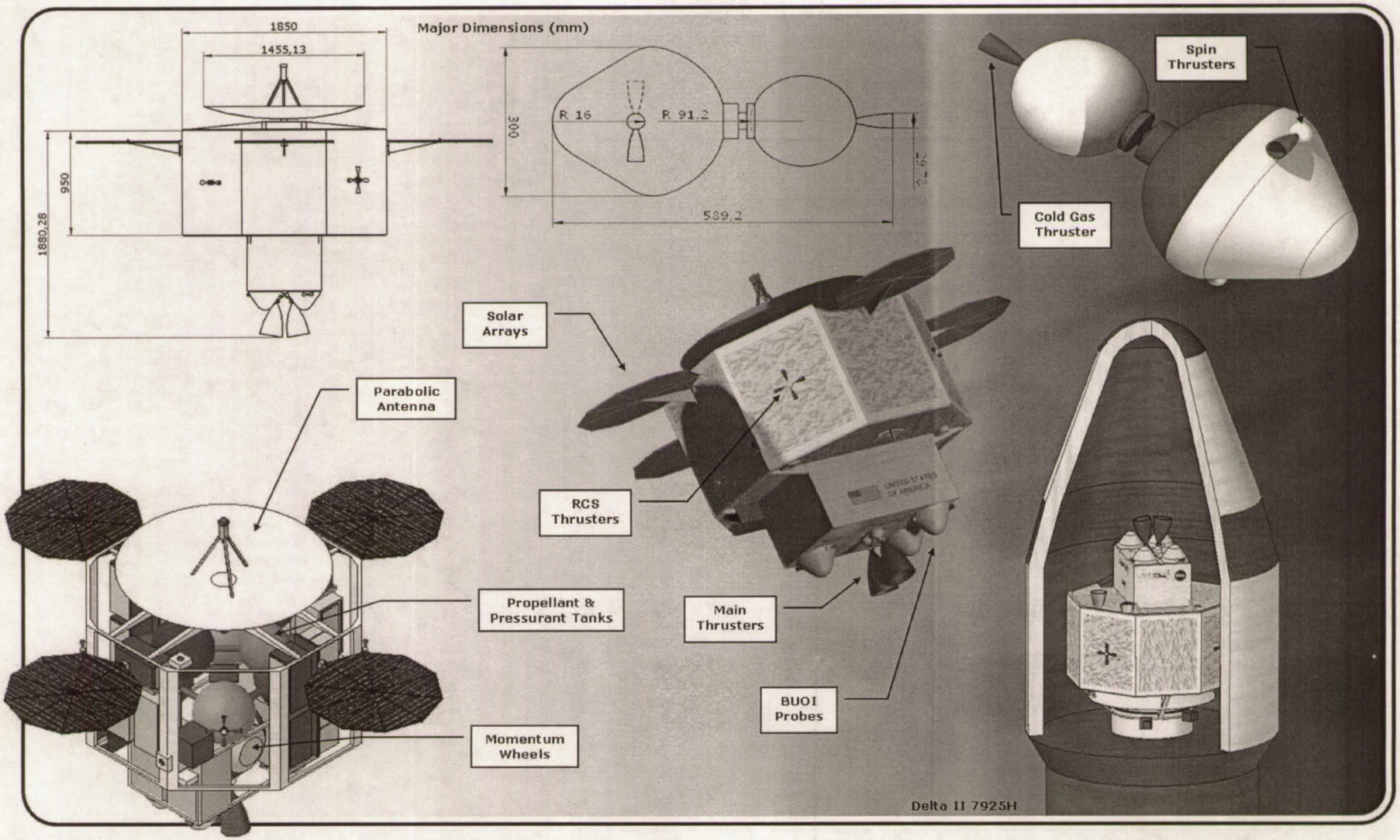
Major Dimensions (mm)
1850
1455,13
950
1880,28
300
R 16
R 91,2
589,2
Spin Thrusters
Cold Gas Thruster
Solar Arrays
Parabolic Antenna
RCS Thrusters
Propellant & Pressurant Tanks
Main Thrusters
BUOI Probes
Momentum Wheels
Delta II 7925H

	Formulation			SUBTOTAL Formulation		Implementation								SUBTOTAL Implementation		TOTAL LIFE CYCLE	
Cost Element	FY08	FY09	FY10	RY$	FY07$	FY10	FY11	FY12	FY13	FY14	FY15	FY16	FY17	RY$	FY07$	RY$	FY07$
Start to Launch + 30 Days (Phases A/B/C/D)																	
Phase A Concept Study	$ 1,538			$ 1,538	$ 1,538											$ 1,538	$ 1,538
Proj. Mgmt/Miss. Analysis/Sys. Eng.		$ 1,549	$ 479	$ 2,028	$ 1,953	$ 1,118	$ 1,646	$ 1,697	$ 778					$ 5,239	$ 4,723	$ 7,266	$ 6,676
Multispectral Imager		$ 2,885	$ 3,607	$ 6,492	$ 6,192	$ 801	$ 1,570							$ 2,372	$ 2,187	$ 8,864	$ 8,378
Near-Infrared Spectrometer		$ 3,630	$ 4,538	$ 8,168	$ 7,791	$ 1,106	$ 2,076							$ 3,183	$ 2,935	$ 11,351	$ 10,726
Laser Rangefinder		$ 2,082	$ 2,602	$ 4,684	$ 4,467	$ 508	$ 1,060							$ 1,568	$ 1,445	$ 6,252	$ 5,912
Magnetometer		$ 1,142	$ 1,428	$ 2,570	$ 2,451	$ 220	$ 521							$ 742	$ 683	$ 3,312	$ 3,134
BUOI Probes		$ 10,826	$ 14,881	$ 25,707	$ 24,500	$ 797	$ 16,439	$ 2,542						$ 19,778	$ 18,000	$ 45,485	$ 42,500
Instr. Integration, Assembly and Test							$ 9,031	$ 5,013						$ 14,044	$ 12,677	$ 14,044	$ 12,677
Subtotal - Instruments		$ 20,565	$ 27,056	$ 47,622	$ 45,401	$ 3,433	$ 30,697	$ 7,556						$ 41,686	$ 37,928	$ 89,308	$ 83,328
Spacecraft bus, cruise stage		$ 8,167	$ 16,840	$ 25,007	$ 23,764	$ 16,840	$ 21,702	$ 22,375						$ 60,917	$ 55,448	$ 85,924	$ 79,212
S/C Integration, Assembly and Test							$ 3,818	$ 4,811						$ 8,629	$ 7,742	$ 8,629	$ 7,742
Other Hardware Elements																	
Launch Ops (Launch + 30 days)									$ 2,462					$ 2,462	$ 2,113	$ 2,462	$ 2,113
Subtotal - Spacecraft		$ 8,167	$ 16,840	$ 25,007	$ 23,764	$ 16,840	$ 25,520	$ 27,186	$ 2,462					$ 72,008	$ 65,303	$ 97,014	$ 89,067
Science Team Support		$ 953	$ 295	$ 1,247	$ 1,201	$ 688	$ 1,013	$ 1,044	$ 1,076					$ 3,821	$ 3,419	$ 5,068	$ 4,620
Pre-Launch GDS/MOS Development								$ 6,685	$ 2,954					$ 9,639	$ 8,453	$ 9,639	$ 8,453
DSN/Tracking									$ 466					$ 466	$ 400	$ 466	$ 400
E/PO, Technology Infusion/Transfer		$ 784	$ 606	$ 1,390	$ 1,330	$ 606	$ 1,250	$ 859						$ 2,715	$ 2,471	$ 4,105	$ 3,801
Planetary Protection								$ 1,432	$ 1,476					$ 2,908	$ 2,534	$ 2,908	$ 2,534
Subtotal Phases A-D before Reserves	$ 1,538	$ 32,017	$ 45,276	$ 78,831	$ 75,187	$ 22,684	$ 60,126	$ 46,459	$ 9,212					$ 138,481	$ 125,230	$ 217,312	$ 200,417
Instrument Reserves		$ 6,170	$ 8,117	$ 14,286	$ 13,620	$ 1,030	$ 9,209	$ 2,267						$ 12,506	$ 11,378	$ 26,792	$ 24,998
Spacecraft Reserves		$ 2,450	$ 5,052	$ 7,502	$ 7,129	$ 5,052	$ 7,656	$ 8,156	$ 739					$ 21,602	$ 19,591	$ 29,104	$ 26,720
Other Reserves	$ 462	$ 986	$ 414	$ 1,861	$ 1,807	$ 723	$ 1,173	$ 3,086	$ 2,025					$ 7,007	$ 6,220	$ 8,868	$ 8,027
Total Phases A/B/C/D	$ 2,000	$ 41,622	$ 58,859	$ 102,481	$ 97,743	$ 29,489	$ 78,164	$ 59,967	$ 11,975					$ 179,596	$ 162,419	$ 282,077	$ 260,163
Launch + 30 Days to End of Mission (Phase E)																	
Mission Operations and Data Analysis									$ 6,043	$ 19,822	$ 19,269	$ 7,224	$ 5,586	$ 57,944	$ 47,156	$ 57,944	$ 47,156
DSN/Tracking									$ 881	$ 908	$ 936	$ 965	$ 758	$ 4,448	$ 3,600	$ 4,448	$ 3,600
E/PO, Technology Infusion/Transfer									$ 295	$ 685	$ 706	$ 728	$ 751	$ 3,165	$ 2,534	$ 3,165	$ 2,534
Subtotal Phase E before Reserves									$ 7,218	$ 21,415	$ 20,911	$ 8,917	$ 7,095	$ 65,557	$ 53,290	$ 65,557	$ 53,290
Reserves									$ 2,166	$ 6,425	$ 6,273	$ 2,675	$ 2,128	$ 19,667	$ 15,987	$ 19,667	$ 15,987
Total Phase E									$ 9,384	$ 27,840	$ 27,185	$ 11,592	$ 9,223	$ 85,224	$ 69,277	$ 85,224	$ 69,277
Launch Services						$ 1,000	$ 36,000	$ 40,000	$ 36,000					$ 113,000	$ 100,096	$ 113,000	$ 100,096
Total NASA Cost	$ 2,000	$ 41,622	$ 58,859	$ 102,481	$ 97,743	$ 30,489	$ 114,164	$ 99,967	$ 57,359	$ 27,840	$ 27,185	$ 11,592	$ 9,223	$ 377,820	$ 331,792	$ 480,301	$ 429,535
														Total Mission Cost		$ 480,301	$ 429,535

											TOTALS	
Cost Element	FY08	FY09	FY10	FY11	FY12	FY13	FY14	FY15	FY16	FY17	RY $	FY07 $
Phase A Concept Study	$ 2,000										$ 2,000	$ 2,000
Additional Phase A (if required)												
Phase B		$ 41,622	$ 11,772								$ 53,394	$ 51,445
Phase C/D			$ 76,576	$ 78,164	$ 59,967	$ 11,975					$ 226,683	$ 206,717
Phase E						$ 9,384	$ 27,840	$ 27,185	$ 11,592	$ 9,223	$ 85,224	$ 69,277
Launch Vehicle/Launch Services			$ 1,000	$ 36,000	$ 40,000	$ 36,000					$ 113,000	$ 100,096
Total NASA Mission Cost											$ 480,301	$ 429,535